

St. Lucie Unit 2
Docket No. 50-389
L-2004-245 Enclosure 2

Enclosure 2

Non Proprietary Version

WCAP-16208-NP dated October 2004, Revision 0
NDE Inspection Length for CE Steam Generator Tubesheet Region Explosive
Expansions

(140 Pages)

Enclosure 1 contains 2.390(a)(4) Proprietary Information

Westinghouse Non-Proprietary Class 3

WCAP-16208-NP
Revision 0

October 2004

NDE Inspection Length for CE Steam Generator Tubesheet Region Explosive Expansions

PA-MS-0036



L E G A L N O T I C E

This report was prepared as an account of work sponsored by the Westinghouse Owners Group (WOG) and Westinghouse Electric Company LLC. Neither the WOG nor Westinghouse Electric Company LLC, nor any person acting on their behalf:

- A. Makes any warranty or representation, express or implied including the warranties of fitness for a particular purpose or merchantability, with respect to the accuracy, completeness, or usefulness of the information contained in this report, or that the use of any information, apparatus, method, or process disclosed in this report may not infringe privately owned rights; or
- B. Assumes any liabilities with respect to the use of, or for damages resulting from the use of, any information, apparatus, method, or process disclosed in this report.

WESTINGHOUSE NON-PROPRIETARY CLASS 3

WCAP-16208-NP

NDE Inspection Length for CE Steam Generator Tubesheet Region Explosive Expansions

T.P. Magee, P.R. Nelson, B.A. Bell, K.E. Coe

Chemistry Diagnostics & Materials Engineering

PA-MS-0036
October 2004

Reviewer:



R.F. Keating, Consulting Engineer
Major Component Replacements and Engineering

Approved:



E.P. Morgan, Manager
Chemistry Diagnostics and Materials Engineering

Westinghouse Electric Company LLC
P.O. Box 355
Pittsburgh, PA 15230-0355

© 2004 Westinghouse Electric Company LLC
All Rights Reserved

COPYRIGHT NOTICE

This report has been prepared by Westinghouse Electric Company LLC for the members of the Westinghouse Owners Group with CE NSSS designs participating in this Group Task, and bears a Westinghouse Electric Company copyright notice. Information in this report is the property of and contains copyright material owned by Westinghouse Electric Company LLC and /or its subcontractors and suppliers. It is transmitted to you in confidence and trust, and you agree to treat this document and the material contained therein in strict accordance with the terms and conditions of the agreement under which it was provided to you.

As a participating member of this Westinghouse Owners Group task, you are permitted to make the number of copies of the information contained in this report that are necessary for your internal use in connection with your implementation of the report results for your plant(s) in your normal conduct of business. Should implementation of this report involve a third party, you are permitted to make the number of copies of the information contained in this report that are necessary for the third party's use in supporting your implementation at your plant(s) in your normal conduct of business if you have received the prior, written consent of Westinghouse Electric Company LLC to transmit this information to a third party or parties. All copies made by you must include the copyright notice in all instances and the proprietary notice if the original was identified as proprietary.

The NRC is permitted to make the number of copies beyond those necessary for its internal use that are necessary in order to have one copy available for public viewing in the appropriate docket files in the NRC public document room in Washington, DC if the number of copies submitted is insufficient for this purpose, subject to the applicable federal regulations regarding restrictions on public disclosure to the extent such information has been identified as proprietary. Copies made by the NRC must include the copyright notice in all instances and the proprietary notice if the original was identified as proprietary.

TABLE OF CONTENTS

TABLE OF CONTENTS	v
LIST OF TABLES	vii
LIST OF FIGURES	ix
Executive Summary.....	xi
1.0 Introduction.....	1-1
1.1 Purpose.....	1-1
1.2 Background	1-2
1.3 Quality Assurance	1-3
2.0 Summary and Conclusions	2-1
2.1 Inspection Lengths Based on the Burst Criterion	2-1
2.2 Inspection Lengths Based on the Leakage Criterion	2-1
2.3 Conservatisms in Results	2-2
3.0 Technical Approach Summary.....	3-1
3.1 Introduction.....	3-1
3.2 Test Methods and Acceptance Criteria	3-1
3.2.1 Sample Description.....	3-2
3.2.2 Pullout Load Tests Methods and Criteria	3-3
3.2.3 Leak Rate Tests Methods and Criteria	3-5
3.2.4 Tubesheet Deflection Analysis Method.....	3-9
4.0 Leak Rate Tests and Results	4-1
4.1 Preliminary Testing.....	4-1
4.2 Room Temperature Testing	4-2
4.3 Selection of Elevated Test Temperature	4-3
4.4 Elevated Temperature Leak Rate Testing.....	4-3
4.5 Statistical Comparison of C* and Task 1154 Data	4-4
4.6 Effect of Temperature and Pressure on Leak Rate	4-5
4.7 Effect of Water Chemistry on Leak Rate.....	4-5
4.8 Evaluation of Leak Rate Data	4-6
5.0 Pullout Load Tests and Results	5-1
5.1 Pullout Screening Test Results	5-1
5.2 Task 1154 pullout tests	5-2
5.3 Analysis of Pullout Test Results	5-3
6.0 Tubesheet Deflection Analysis	6-1
6.1 Finite Element Model Analysis	6-1
6.2 Dilation Correction for Burst	6-2
6.3 Dilation Correction for Leakage	6-3
7.0 Other Factors.....	7-1

7.1	Vertical Constraint Evaluation.....	7-1
7.1.1	Summary.....	7-1
7.1.2	Vertical Constraint Determination for Plant CI, Plant CE and Plant CG.....	7-1
7.1.3	Vertical Constraint Determination for Plant CF, Plant CD and Plant N.....	7-3
7.2	EDM Cutting Effects.....	7-4
7.3	Expansion Taper.....	7-4
7.4	NDE Axial Position Uncertainty.....	7-5
7.5	NDE Characterization Of Tubesheet Hole Surface Roughness.....	7-7
8.0	Definitions.....	8-1
9.0	References.....	9-1
APPENDIX A	SUMMARY OF ROOM TEMPERATURE LEAK TEST RESULTS.....	A-1
APPENDIX B	SUMMARY OF ELEVATED TEMPERATURE LEAK TEST RESULTS.....	B-1
APPENDIX C	LEAK RATE VS TIME PLOTS AT SLB.....	C-1

LIST OF TABLES

Table 2-1: Leakage Based Inspection Length Including Tubesheet Deflection and NDE Corrections for All CE Designed Steam Generators	2-4
Table 3-1: Test Specimens	3-10
Table 3-2: Test Conditions	3-10
Table 4-1: Summary of Elevated Temperature Leak Rate Tests	4-9
Table 4-2: Data Used in the Regression Analysis	4-11
Table 4-3: Regression Results for Equation 2 Model Using C* & 1154 Data	4-12
Table 4-4: Leak Rate vs. Temperature Tests	4-13
Table 4-5: Data Used To Estimate Effect of Temperature and Pressure on Leak Rate	4-14
Table 4-6: Transformed Leak Rate Data	4-15
Table 4-7: Generation of Sample with Replacement Data Set	4-16
Table 4-8: Uncorrected Joint Lengths that Meet Leakage Criterion for Each Plant	4-17
Table 5-1: Summary of Screening Pullout Tests	5-5
Table 5-2: Rough Bore Pullout Test Data from Previous Test Programs (Room Temperature, Ambient Internal Pressure)	5-6
Table 5-3: Smooth Bore Pullout Test Data from Previous Test Programs	5-7
Table 6-1: Maximum Pullout Load for 3NODP	6-6
Table 6-2: Tubesheet Deflection Analysis Results, Reduction in Contact Load for Plant CF2 & CF3 and Plant CD Steam Generators	6-7
Table 6-3: Tubesheet Deflection Analysis Results, Reduction in Contact Load for Plant CI Steam Generators	6-8
Table 6-4: Tubesheet Deflection Analysis Results, Reduction in Contact Load for Plant N Steam Generators	6-9
Table 6-5: Tubesheet Deflection Analysis Results, Reduction in Contact Load for Plant CG Steam Generators	6-10
Table 6-6: Tubesheet Deflection Analysis Results, Reduction in Contact Load for Plant CE1 Steam Generators	6-11
Table 6-7: Tubesheet Deflection Analysis Results, Reduction in Contact Load for Plant CE3 Steam Generators	6-12
Table 6-8: Burst Based Inspection Length Including Tubesheet Deflection and NDE Corrections For All CE Designed Steam Generators	6-13
Table 6-9: Effect of Tubesheet Deflection for Plant CF and Plant CD Steam Generators	6-14
Table 6-10: Effect of Tubesheet Deflection for Plant N Steam Generators	6-15
Table 6-11: Effect of Tubesheet Deflection for Plant CG Steam Generators	6-16
Table 6-12: Effect of Tubesheet Deflection for Plant CE1 Steam Generators	6-17
Table 6-13: Effect of Tubesheet Deflection for Plant CE3 Steam Generators	6-18
Table 6-14: Effect of Tubesheet Deflection for Plant CI Steam Generators	6-19

Table 6-15: Inspection Length Based on Leakage.....6-20
Table 7-1: NDE Test Sample Identification, BET Positions and Flaw Positions 7-8
Table 7-2: Summary of NDE Uncertainties for Indications Below the TTS in Explosive
Expansions7-10
Table 7-3: Random Noise Measurements in Tubesheet 7-11
Table 7-4: Random Noise Sample Ranking.....7-12

LIST OF FIGURES

Figure 3-1: Drawing Showing Test Sample Dimensions.	3-11
Figure 3-2: Windsor Load Cell Test Controls and Data Plotter	3-12
Figure 3-3: Leak Test Equipment Schematic.....	3-13
Figure 4-1: Comparison of Sample 1 Room Temperature Leak Test Results with CEOG 1154 (at SLB Pressure).	4-18
Figure 4-2: Plot of Leak Rate vs. Joint Length at 600°F, $\Delta P = \text{SLB}$	4-19
Figure 4-3: Sample 2 (Joint Length=1.5") Temperature Dependency.	4-20
Figure 4-4: Sample 3 (Joint Length=4") Temperature Dependency.	4-21
Figure 4-5: Sample 6 (Joint Length=2.25") Temperature Dependency.	4-22
Figure 4-6: Sample 6 (Joint Length=3", P=NODP) Temperature Dependency.	4-23
Figure 4-7: Cumulative Distribution of Temperature and Pressure Effects on Leakage. (Used to Estimate the Effect on Leak Rate.).....	4-24
Figure 5-1: Pullout Force for 48 mil Wall Rough Bore Samples from the Boston Edison Steam Generators, CEOG Task 1154 and Sample 1. (The tests that used tubes with 42 mil data were scaled to 48 mil wall. Process adjustment made to Task 1154 data).....	5-8
Figure 5-2: Pullout Force for 42 mil Wall Rough Bore Samples from the Boston Edison Steam Generators and CEOG Task 1154. (The tests that used tubes with 48 mil data were scaled to 42 mil wall. Process adjustment made to Task 1154 data).	5-9
Figure 5-3: Pullout Force for 42 mil Wall Smooth Bore Samples from CEOG Task 1154, Ringhals Samples and Samples 3 and 4.....	5-10
Figure 7-1: Miscellaneous Views of Upper Bundle Support Structures.....	7-13
Figure 7-2: Bend Region Tube Supports.	7-14
Figure 7-3: Vertical and Horizontal Strip Arrangement.	7-15
Figure 7-4: Vertical Grid Geometry.	7-16
Figure 7-5: Results of EDM Cut Through the Tube Wall and Partially into the Tubesheet.	7-17

EXECUTIVE SUMMARY

All pressurized water reactor (PWR) licensees have Technical Specifications, a.k.a. Tech Specs, which govern the surveillance of the steam generator (SG) tubes. The Tech Specs do not typically prescribe the nondestructive examination (NDE) methods or the locations where specific methods are to be applied. The selection and application of supplemental techniques such as rotating pancake coil technology probes has been specified by the licensee based on ensuring tube integrity in accordance with the licensing basis and satisfying the requirements of NEI 97-06. Inspecting tubes with specialized probes is generally more time consuming than with bobbin coil probes, hence the slower probes have not been typically applied of the entire length of the tube within the tubesheet that is subject to scheduled inspection. Limiting the extent of the supplemental inspections is typically based on the degradation assessment and a tube integrity evaluation. Such evaluations have shown that not inspecting portions of the tube within the tubesheet would be inconsequential to the structural and leak rate margin during normal operation and postulated accident events. The information contained in this report supports an inspection basis for that portion of the tube explosively expanded within the tubesheet for plants with Combustion Engineering (CE) designed SGs. The analysis demonstrates that degradation below a specified threshold within the tubesheet designated as C* is not a concern regarding the structural or leakage integrity of the tube.

Steam generator tube circumferential and axial primary water stress corrosion cracking (PWSCC) has been detected in the tubesheet region below the tube expansion transition in CE designed units. This report provides the recommended inspection length below the tube to tubesheet joint expansion transition for qualified eddy current techniques to determine if a postulated crack population leakage is within limits. All cracks that are detected above the recommended inspection length are recommended to be plugged or repaired by current requirements, but an undetected population of cracks is assumed to exist and accumulate in uninspected region from the time that PWSCC is detected in the expansion transition area until the end of steam generator life. The detection and removal from service of cracks in the defined inspection length precludes any structural (tube burst by exit from the tubesheet) concern. Furthermore, testing and analysis results indicate that a postulated, extremely severe, undetected flaw population below the C* distance would not be expected to be of significant concern during normal operation or postulated accident conditions.

The recommended inspection length, i.e., C*, is based on results from a conservative test and analysis program, supplemental to that of Reference 4, to ensure that the requirements for tube structural and leakage integrity provided in NEI 97-06, Reference 2, are met. A description and explanation of the testing and analysis methods are provided in this report. [

]^(a,c,e) The recommended inspection lengths are provided in the following table.

Plant	Leak Rate Based Inspection Length Corrected for Dilation and NDE (in.)
Plant CI	11.4
Plant N	10.1
Plants CF & CD	10.4
Plant CG	11.6
Plant CE1	10.4
Plant CE3	11.6

1.0 INTRODUCTION

1.1 PURPOSE

Steam generator tube circumferential and axial primary water stress corrosion cracking (PWSCC) has been detected in the tubesheet region below the tube expansion transition in Combustion Engineering (CE) designed units. The Westinghouse Owners Group (WOG) has conducted a project for the following plants to develop a technical basis for an inspection length in the tubesheet region:

- Plant CI
- Plant N
- Plant CG
- Plant CE, 2 Units
- Plant CF, 2 Units
- Plant CD

The purpose of the testing and analysis program was to develop an inspection length that provides a reasonable assurance of structural and leakage integrity for the portion of the tube within CE-designed tube-to-tubesheet expansion joints.

This report provides the recommended inspection length below the tube to tubesheet joint expansion transition for qualified eddy current techniques to determine if the postulated crack population leakage (below the inspection length) is within required limits. The inspection length developed in this report is based on the limiting leakage criteria so that a pre-determined assumed flaw population is conservatively postulated to be leaking at the rate measured in testing or extrapolated from test measurements. The leak based inspection length is dependent on the amount of tubesheet flexure at main steam line break conditions. Tubesheet flexure is plant design dependent and the recommended inspection lengths provided in this report have been determined on the basis of plant design using the tubesheet radial location corresponding to the greatest flexure.

The recommended inspection length provided herein is based on the most conservative flaw population and flaw characterization assumptions that all tubes are degraded by 100% throughwall 360° circumferential cracks. All cracks that are detected above the specified inspection length are recommended to be plugged or repaired, but an undetected population is assumed to exist and to accumulate below the inspection length from the time that PWSCC is first detected in the expansion transition area until the end of anticipated steam generator life. The detection and removal from service of cracks in the defined inspection length precludes any structural concern, i.e., tube burst by exit from the tubesheet. This report provides the basis to account for undetected flaw population leakage, assuming accident conditions, in condition monitoring and operational assessment determinations.

The recommended inspection length, entitled C*, is based on results from a conservative test and analysis program to ensure that the requirements for tube structural and leakage integrity provided in NEI 97-06 are met. A description and explanation of the testing and analysis methods are provided in this report. Results from parametric testing of chemistry effects on leak rate conducted in supplementary tests indicate that high temperature deoxygenated test water yields results typical of those using simulated reactor coolant. Burst test results are unaffected because of the test parameters are combined for use in the development of the recommended inspection length. This report provides the technical basis for the recommended inspection length.

1.2 BACKGROUND

Beginning in 1961, Combustion Engineering pioneered the use of explosive expansion for steam generator tubesheet joints and termed it "expansion." The desired design features were to provide an efficient method for closing the tube to tubesheet gap over the full length with significant pullout strength, leak tightness and without imparting excessive residual stresses in the tubes.

Tubesheets were, at that time, some of the thickest forged plates for any application in the world. Tubesheet hole drilling was considered to be a time-consuming process with a high potential for inspection rejection and manufacturing rework. [

](a,c,e)

Because the bobbin coil probability of detection (POD) for flaws in the tubesheet region is not currently qualified in accordance with EPRI standards, POD is assumed to be high only for relatively deep cracks. In general, industry practice is to assume undetected flaws are present only if the particular flaw mechanism is believed to be present. The case presented in this report is that the presence of undetected flaws in the tubesheet region below the threshold distance criterion is inconsequential from a tube burst and leakage standpoint. Reasonable assurance of detection of flaws in the region above the threshold distance will be provided through the use of a qualified detection technique (e.g., +Point™).

In the late 1990s, tubes in Babcock and Wilcox (B&W) designed plants were discovered to have cracks in the tubesheet region, leading the United States Nuclear Regulatory Commission (NRC) to issue of an Information Notice (IN 98-27) alerting the pressurized water reactor (PWR) industry to the events. The B&W tube to tubesheet joint design is an open crevice with a short

hard roll near the tube end, which has limited applicability to the CE design, but highlighted the need to review inspection practices in this region.

Alternate repair criteria designated as W* were developed by Westinghouse in 1992, Reference 13, to address cracks in the tubesheet region for the Westinghouse explosive tube expansion (WEXTEX) tube to tubesheet joint design. The application of W* provides for leaving axial cracks in-service if they meet the W* criteria. The WEXTEX joint is similar in design to the CE expansion joint.

The CE Owners Group (CEOG) decided in the late 1990s to similarly address tube inspection in the tubesheet region. CEOG Task 1154, Reference 4, was a test program that provided a basis for the inspection length that preceded the C* work reported herein. In 2002, several CE plants submitted technical specification changes to the NRC staff for establishing an inspection length below the expansion transition based on the Task 1154 results. The NRC staff reviewed the submittals and responded with requests for additional information (RAIs). The C* test program results are supported by some, but not all, of the results from the CEOG Task 1154 test program. Some of the Task 1154 pull test results were applicable, but the high temperature leak rate results are superseded by the C* results as a consequence of tests comparing the effects of reactor coolant system (RCS) chemistry on leakage.

The NRC issued Generic Letter (GL) 2004-01, Reference 5, directing utilities to provide information to address their concerns regarding tubesheet region inspection. The generic letter is intended by the NRC staff to include addressing the inspection adequacy with regard to the tubesheet region for those units that have experienced primary water stress corrosion cracking (PWSCC) in the tube expansion transition. Although the inspection for stress corrosion cracking (SCC) below the top of the tubesheet has been a topic of ongoing discussion between the industry and the NRC, available technical information based on analysis and supported by testing programs has shown that compliance with the applicable performance criteria is highly likely.

This report provides a recommended inspection length below the top of the tubesheet for plants with CE explosively expanded tube to tubesheet joints that have detected stress corrosion cracking in the tubesheet region below the tube expansion transition. The recommended inspection length was developed to ensure that the structural and leakage criteria of NEI 97-06 are met. The recommended tubesheet region inspection length determined for each unit is reported in Sections 2 and 6 of this document.

1.3 QUALITY ASSURANCE

This work was completed under the requirements of the Westinghouse Quality Assurance Program (Reference 1).

2.0 SUMMARY AND CONCLUSIONS

The recommended inspection length, i.e., C^* , is based on results from a conservative set of tests, using typical tube to tubesheet joint specimens and test water, and an analysis program to ensure that the performance criteria of NEI 97-06, Reference 2, for tube structural and leakage integrity are met. The inspection length developed for leakage bounds the inspection length for structural integrity. [

$]^{(a,c,e)}$ A

summary of the results are provided in this section.

The detection and removal from service of cracks in the defined inspection length precludes any structural concern regarding the tube pulling out of the tubesheet. Moreover, the total leakage from an undetected flaw population based on postulated accident conditions is accounted for to assure that the leakage criterion is met for condition monitoring and operational assessment determinations.

[

$]^{(a,c,e)}$

2.1 INSPECTION LENGTHS BASED ON THE BURST CRITERION

The required joint length, based on burst criteria, was determined both for gun-drilled (rough bore) and BTA (smooth bore) tubesheet holes. The burst based length is bounded by the required joint length for leakage, but was determined to demonstrate the length necessary to meet the industry requirements specified in Reference 2 (see Sections 5.0 and 6.0).

The tube-to-tubesheet joint reaction force required to resist the tube from being forced from the tubesheet was determined as the force recorded in pullout load tests. The tests, which were based on the burst criterion, determine the actual force at the point of overcoming the friction force holding the tube in the tubesheet. In some C^* tests, the test was terminated without tube movement after 3NODP was achieved. The tests terminated at 3NODP support the conclusions of the lengths provided in this report but are not useful as data points in determining contact force as a function of joint length.

The results of the pull force tests have been organized into three data sets representing the three CE joint designs: 48 mil tube wall rough bore; 42 mil tube wall rough bore; and 42 mil tube wall smooth bore. The 3NODP burst limit based joint length uncorrected for tubesheet dilation and NDE positional uncertainty ranges from [$]^{(a,c,e)}$

2.2 INSPECTION LENGTHS BASED ON THE LEAKAGE CRITERION

The inspection lengths developed in this report are based on the limiting leakage criterion so that a specified assumed flaw population below the inspection length is conservatively postulated to be leaking at the rate measured in testing or extrapolated from test measurements. The leak based inspection length is dependent on the amount of tubesheet flexure at SLB conditions. Tubesheet

flexure is plant design dependent and the recommended inspection lengths provided in this report have been determined on a plant specific basis. The inspection lengths determined by extrapolation of leak test results are corrected analytically to include the effects of the limiting tube hole dilation due to tubesheet bowing and adjusted to account for NDE probe position uncertainty. The results are derived from bounding single tube leak rate test results.

The recommended inspection length provided is based on the most conservative assumed crack population; all tubes are assumed to be degraded by 100% throughwall 360° circumferential cracks, all located immediately below the inspected length of tube. To address potential primary-to-secondary leakage from indications below the C* elevation, an undetected population is assumed to exist and accumulate in the uninspected region from the time that PWSCC is detected in the expansion transition area until the end of SG life that is bounded by the evaluation assumptions.

The recommended inspection lengths are provided in Table 2-1 and range from []^(a,c,e)

2.3 CONSERVATISMS IN RESULTS

There are a number of conservatisms inherent in the evaluations documented in this report. The following is a non-inclusive list regarding the prediction of leakage from postulated affected tubes:

[

]^(a,c,e)

The following are a few conservatisms inherent in the pullout force analysis, although the results are bounded by the C* distance established from leak rate considerations:

[

]^(a,c,e)

Table 2-1: Leakage Based Inspection Length
Including Tubesheet Deflection and NDE Corrections
for All CE Designed Steam Generators

Plant	Leak Rate Based Inspection Length Adjusted for TS Dilation (inches)	Leak Rate Based Inspection Length Adjusted for TS Dilation and NDE (inches)
Plant CI	11.1	11.4
Plant N	9.8	10.1
Plants CF & CD	10.1	10.4
Plant CG	11.3	11.6
Plant CE1	10.1	10.4
Plant CE3	11.3	11.6

3.0 TECHNICAL APPROACH SUMMARY

3.1 INTRODUCTION

This section provides a summary of:

- The approach used for collecting and evaluating the data from which the recommendations are derived.
- The acceptance criteria for the results and bases for the acceptance criteria
- Apparatus, test procedures, technique description, and data.

Detailed test apparatus, test procedures, technique description, and data tables are provided elsewhere, as described. All materials were procured and methods/procedures were executed under Westinghouse quality requirements, Reference 1.

3.2 TEST METHODS AND ACCEPTANCE CRITERIA

Acceptable joint length was determined by testing for two categories of concern: pullout load and leak rate. Pullout load and leak rate testing data were compared to industry accepted criteria (Reference 2).

The tube-to-tubesheet joint length needed to ensure that both pullout (burst) and leakage criteria are met was determined in this project. The length needed to ensure both criteria are met was dominated in all cases by the threshold length defined by the leakage criterion.

The leak rate criterion is based on the generic allowable leakage technical specification limiting condition for operation of 0.5 gpm per steam generator. Operational assessment calculations include assumptions for undetected flaw populations and determine acceptable plant run-time based in part on acceptable EOC leakage. The criterion is conservatively limited to one-fifth of the total allowable leakage, or 0.1 gpm, for this single type of flaw (tubesheet region cracking). The joint length leak rate (determined by testing) multiplied by the number of tubes assumed to be defective that results in a leak rate less than or equal to the leak rate criteria of 0.1 gpm is the plant-specific threshold length for leaks.

The limiting conditions for the leak rate criterion are based on a conservative assessment of conditions during a main steam line break (SLB) event. Leak rate data was evaluated at a pressure of 2560 psid and 600°F. The pressure value of 2560 psid corresponds to the pressurizer safety valve setpoint plus 3 percent for valve accumulation less atmospheric pressure in the faulted steam generator (Reference 3). This pressure differential represents the pressure that would be obtained during a main steam line break due to total depressurization of the faulted steam generator with reactor coolant pressure rising to the setpoint of the reactor coolant system safety valves due to the operator failing to terminate safety injection. In order to reach this value for a main steam line break, the pressurizer PORVs would have to fail or be unavailable and the operator must fail to terminate safety injection flow. The temperature value of 600°F was based

on approved methodology and conservative use of preliminary leak rate test results, as is described in Section 4.3.

The normal operating pressure differential (NODP) varies significantly from plant to plant. The choice of NODP for leak test evaluations was chosen, along with testing at SLB pressure, to provide the widest range of expected pressures. A NODP of 1270 psid was used.

3.2.1 Sample Description

The tube mockup assemblies consisted of 0.750" OD Alloy 600MA tube specimens explosively expanded into an 8" thick by 1.625" OD tubesheet simulating collars fabricated from SA-508, Class 3, carbon steel. Approximately 6" of tube length extended out from the secondary face of the tubesheet as illustrated on Figure 3-1. Samples that had been archived from the CEOG Task 1154 program, Reference 4, as well as two samples that had been provided to Plant CE3 for use as NDE standards, none of which had ever been leak or pullout tested, were used as laboratory test specimens in this program. The archived samples were used instead of manufacturing new samples with the intent of providing sample consistency between the two programs.

The tubing material properties were at the high end of the standard CE specification for yield strength (Reference 4), i.e., 54 ksi versus a standard specification value of 35-55 ksi for CE designed SG tubes. Tube wall thicknesses of 0.042 and 0.048 inch were tested. Two different tubesheet drilled hole finishes were tested: one representing the gun-drilled process (drilled); and one representing the BTA process (drilled and reamed). The first is called "rough bore" in this report and is representative of Plant CI, Plant CD, Plant N, Plant CF 2, Plant 3 and Plant CE1. The second type is referred to as "smooth bore" and is representative of Plant CE3 and the Plant CG replacement steam generator tubesheet hole surfaces. The tubes were expanded into the simulated tubesheets (collars) using the standard CE fabrication method. A detailed description of the manufacturing processes is provided in Reference 4.

Table 3-1 lists the sample assemblies that were tested in this program. Samples 1 through 7 were initially numbered as part of the Reference 4 program and were renumbered for this study. Table 3-1 provides a cross-reference listing of both numbers; however, the samples are referred to herein by the numbers assigned for this program.

[

](a,c)

[

$$J^{(a,c)}$$

The test joint length was defined as the distance from the TTS to the uppermost edge of the EDM cut. [

$$J^{(a,c,e)}$$

3.2.2 Pullout Load Tests Methods and Criteria

The presence of the tubesheet precludes bursting of axially degraded tubes. For tubes with circumferential degradation, e.g., cracking, within the tubesheet, burst is resisted by the nondegraded ligament and the interference load between the tube and the tubesheet resisting axial motion, or pullout, of the tube from the tubesheet. For a tube postulated to be severed within the tubesheet, only the pullout load prevents burst. For most tube in the bundle, geometric features would also prevent the pullout condition, but that is conservatively neglected for structural evaluation purposes. The intent of the pullout tests was to determine the sound length of tube-to-tubesheet engagement needed to resist the axial force associated with internal pressure in a severed tube. The pullout load associated with the three times the NODP criterion of Reference 2 bounds the load associated with 1.4 times the SLB differential pressure (1.4 x 2560 psi) for the CE designed SGs of this study.

Since the CEOG Task 1154 program had firmly established that the leak rate based inspection length bound the pullout based inspection length, pullout tests were conducted as part of this program only to confirm that a tube that was completely severed a given distance below the top of the expansion transition would not be ejected from the tubesheet. Pullout loads were only applied up to an equivalent of 3NODP. Once it was demonstrated that a given joint was able to withstand the 3NODP load, it was available for further testing at shorter joint lengths. In all cases, pullout testing was only conducted after all leak rate testing had been completed.

The purpose of the pullout testing was to demonstrate that a tube joint could withstand a 3NODP load. The pullout force is dependent upon the contact force, contact area, coefficient of friction, etc., that is, the tribology. It would be unrealistic and excessively conservative to apply the load by an external tensile force only. [

$$J^{(a,c,e)}$$

The end cap load increases proportionately with the internal pressure. About 70% of the internal pressure is transmitted to the tube-tubesheet hole interface as contact pressure. It was initially thought that the friction forces would exceed the blowout forces, thus the lowest plant NODP would bound the other plants. However, for the short engagement lengths tested, this was not the case and the plan had to be changed. Initially, the lowest NODP among the active participants in this program at the time (which did not include Plant CF) was chosen for the internal pressure, while the highest NODP was chosen for the tensile load. In this case Plant CE1 had the lowest NODP (based on a 2000 Operational Assessment) of 1270 psi, while Plant CD had the highest NODP (based on Refueling Outage 12 Uprate calculations) of 1435 psi. The equivalent tensile load to 2NODP is 1292 lb_f using a tubesheet hole diameter of 0.757 inch. However, when one of the samples (sample 1), with a one inch joint length, had a blowout at a pressure of 1660 psig, it was reasoned that the end-cap pressure dominates the increase in contact pressure, thus the remaining pullout tests were conservatively conducted with an internal pressure of 1435 psig (Plant CD value) instead of 1270 psig. The one inch joint length at which the blowout occurred was well below the lengths discussed in Section 6.

Pullout tests were conducted at room temperature. Under accident conditions, the loss of contact force due to tubesheet hole dilation is partially offset by the increase in contact force by differential thermal expansion. The differential thermal expansion between Alloy 600 tubing and the carbon steel tubesheet is a meaningful factor in the joint force, but not as significant as the increase in contact stress due to pressure internal to the tube. Transient temperature changes during a design basis SLB may play a role in lessening the effect resulting from initial SG pressure blowdown and the associated RCS cooling. However, the thermal capacitance of the tubesheet and the RCS reheat after several minutes in to the worst case transient will re-establish the joint force due to the greater expansion of Alloy 600 tubes. Tubesheet dilation is further addressed in Section 6.

Pullout tests were conducted in the Westinghouse laboratory facilities in Windsor, Connecticut, using calibrated load cells. Pullout testing is reported in Section 5 as the force required for first movement of the tube in the tubesheet hole against the static friction. Data is reported in units of pounds-force (lb_f). Mockups with varying engaged lengths of tubing were tested in accordance with the References 7 and 8 procedures. The engaged lengths for mockups tested was between 1 and 6 inches.

Figure 3-2 illustrates the data logging and process control equipment used in the pullout tests. For the pullout tests, a retention plate with a threaded hole was used to secure the upper end of the tube to the load cell and a similar plate was used to secure the collar to the crosshead. Threaded plugs that had a means of allowing nitrogen to enter and exit the tube were welded to the upper end of the tube and to the lower end of the collar. The threaded portion of the plugs was screwed into the threaded hole of the two retention plates. [

]^(a,c) A digital data acquisition system was used to record load versus crosshead displacement as well as internal tube pressure. After the specimen was secure in the test machine, loads were applied slowly until either the maximum load was achieved or the severed

tube moved within the tubesheet, whichever came first. The load at which first slippage of the tube in the tubesheet occurred was noted and recorded.

3.2.3 Leak Rate Tests Methods and Criteria

Leak rate from the primary to the secondary side of the tube-to-tubesheet joint is a function of the differential pressure, the length of the crevice, the viscosity of the fluid, water or a water and steam mixture, and the resistance of the crevice. In Reference 24 the resistance is embodied in a parameter referred to as the loss coefficient. A parallel parameter is the permeability. The loss coefficient is a function to the contact pressure between the tube and the tubesheet. Empirical data are necessary for understanding the leak rate as a function of joint length and the other parameters. During a SLB event, the maximum differential pressure (2560 psi, the flow forcing function) will occur when the secondary side pressure is approaching atmospheric pressure. Any primary coolant leaking from the tube-to-tubesheet crevice to atmospheric pressure will flash to steam and a choked flow condition could occur. The choked flow condition is not considered in this project but is likely an additional conservatism in the development of the threshold joint length. The purpose of these tests was to determine a sufficient joint length that satisfied the criteria.

The leak rate criterion is based on the generic allowable leakage technical specification limiting condition for operation of 0.5 gpm per steam generator. Operational assessment calculations include assumptions for undetected flaw populations and determine acceptable plant run-time based in part on acceptable EOC leakage. To allow for leakage from other defect flaw types, as well as potential tubesheet region cracking, particularly in operational assessment calculations, the criteria is conservatively limited to one-fifth of the total allowable or 0.1 gpm for indications below the C* length. The joint length leak rate (determined by testing) multiplied by the number of tubes assumed to be defective that results in a leak rate less than or equal to the leak rate criteria of 0.1 gpm is the plant-specific threshold length for leaks.

Each tube has two joints – hot leg and cold leg side. The number of tubesheet joints varies considerably between plants from approximately 10,000 joints in each Plant CI steam generator to more than 22,000 joints per Plant CE steam generator. PWSCC is a temperature driven cracking mechanism and hot-side joints will be the predominate number of tube joints affected over time. On this basis, only the hot-side joints are considered in the development of threshold length for inspection. Leak rate is considered cumulatively for all tube joint leaks in the steam generator. Therefore, the test results provided on a single joint basis are multiplicative of the number of tubes assumed to be leaking. In the development of the leak rate criteria, in order to ensure that the criteria are met in lieu of inspection by rotating probe below the threshold length it is assumed that 100% of all tubes could have a throughwall leak that leaks at the rate determined in the testing.

Section 10 of the EPRI Steam Generator In Situ Guidelines (Reference 9) calls for a correction to account for the difference in crack opening area and thermal hydraulic conditions for the flow at room and operating temperature. The flaws in this program were 360°, 100% throughwall EDM cuts without ligaments; thus the crack opening room to operating temperature area ratio is essentially equal to 1. As a conservatism, this program did not take credit for the potential for

reduced leak rates that would result from the choked flow exiting the tube-tubesheet annulus. Thus, as a conservatism, leak rates were not adjusted for accident conditions.

Leak rate testing was used to determine the joint length, i.e. the threshold length for leakage, for acceptable leakage at SLB conditions from through-wall defects located within the tubesheet region. This phase of the program used the archived tube-tubesheet joint mockups from the Task 1154 program. Most of the tests were conducted at the Windsor, Connecticut, facility. However when it had been shown that there was a significant difference in leak rates between the present program and the Task 1154 program, additional leak rate tests were conducted at the Westinghouse Science and Technology Department (STD) in Churchill, Pennsylvania.

3.2.3.1 Windsor Leak Rate Testing

Test procedures were developed and used for both types of tests, References 7 and 8. The test rig was constructed to provide simulated primary water (or deionized water) to the inside of the test sample tube. This rig had the ability to provide water to the primary side of the sample at a rate [

]^(a,c) Figure 3-3 presents a full schematic of the equipment used to perform elevated temperature leak testing. The sample was placed inside a vessel that had penetrations to [

]^(a,c)

A significant difference from the CEOG Task 1154 work was that simulated primary water was used instead of deionized water. The simulated primary water that was used approximated mid-cycle reactor coolant system chemistry. This water contained [

]^(a,c)

Leak rate was measured by monitoring the volume of room temperature liquid entering the sample. This was accomplished by [

]^(a,c) In the case where a very small leak was anticipated, the system itself was leak checked by pressurizing the system, closing it off and watching for any drop in pressure over a period of up to two hours. Table 3-2

provides a summary of the pressures that were used for leak testing. The SLB pressure was a common design pressure for most of the operating plants and includes a small correction for relief valve reaction. The intermediate pressure was chosen as the mid-point between SLB and NODP.

3.2.3.2 STD Leak Rate Testing

The testing at STD had two objectives: (1) Determine the difference in leak rate that was attributable to the use of primary water vs. the use of oxygenated deionized water, and (2) Assess whether there was a difference in results that might be attributable to the methods and equipment used at the STD and Windsor facilities.

Samples 7 and 37, with joint lengths of 2 and 3.5 inches, respectively, were provided to STD for testing using STD equipment and methods, but using the same test conditions that were used in the Windsor labs. The Reference 10 procedure was developed to guide the testing.

Some of the more significant differences between testing performed at the two laboratories include:

[

](a,c,e)

Deionized water was used during some of the testing of the specimens. The deionized water came from the house system that and was further treated with a lab system containing a mixed ion exchange bed and an organic removal cartridge. The pH, conductivity, and dissolved oxygen content of the deionized water were measured prior to testing. The deionized water was contained in a stainless steel vessel. After equilibration with air, the vessel was pressurized with a 2 to 3 psig nitrogen overpressure to allow for consistent head for the high pressure injection pump. The oxygen concentration measured in the deionized water from the storage vessel was always greater than 5 ppm (5000 ppb). Based on the partial pressures of oxygen and nitrogen in the system, and the room temperature Henry's law constants for these gases, the calculated dissolved oxygen concentration was 6 cm³ (STP)/kg water and the dissolved nitrogen

concentration was 15 cm³ (STP)/kg water.

[]^(a,c)

Some of the STD tests were conducted after exposure to a simulated secondary side AVT water to “condition” it (reduce oxides that might be on the sample). [

] ^(a,c,e)

[

] ^(a,c,e)

The most significant difference between the Windsor and STD laboratory procedures is perhaps the conditioning of the samples in simulated secondary water. The Section 4 test results demonstrate a significant change in leak rate from the conditioning, as shown by the pre- and post-conditioning leak rates measured at STD.

The location of the Windsor thermocouple provided a measurement of the tubesheet temperature near the leakage, while the STD thermocouple provided a primary side coolant temperature. Both methods attempted to measure the temperature of the leakage through the EDM notch. The tubesheet temperature would be expected to somewhat lower than the primary side temperature; thus for the same temperature value, the Windsor tests would actually be conducted at a slightly hotter temperature. This is consistent with the results, which showed that the Windsor tests were measured to leak at a lower rate than the STD tests.

The other factors may have some secondary significance, such as a minor difference in viscosity due to minor differences in water chemistry or differences in dissolved oxygen. Measuring the liquid that enters the sample or condensing the leakage from the sample is not a significant difference. The measurement of leakage by monitoring pressure increases in a closed secondary environment is not expected to provide any significant difference from the other methods as long as the range of pressure increase is kept small, 100-200 psi.

3.2.4 Tubesheet Deflection Analysis Method

A finite element analysis (FEA) was performed to calculate the effect of the tubesheet deflection (flexure) on the contact load between the tube and tubesheet. Tubesheet hole dilation effects were calculated using a single tube model and tubesheet stresses for the Design Differential pressure. The FEA provided a direct output of the tube/tubesheet interface loads, which represented a reduction to the contact loads from tube expansion. The interface loads vary from a maximum value at the tubesheet surface to approximately zero at the mid-surface, and compressive below the neutral axis. This variation was included in the combination with the expansion loads.

The tube pullout tests were used to establish the contact load for the tube expansion. The pullout tests for the tubesheet collars for the rough bore condition, at room temperature, with and without pressure were used. The average load was determined by normalizing the load to a one-inch engagement length and averaging the total data. The contact load was calculated from the pullout load and the coefficient of friction. A coefficient of friction of $[\mu]^{(a,c,e)}$ was used based on historical precedence, e.g., Reference 12. The calculated contact load was uniformly applied over the full tubesheet thickness. The net contact load results from subtracting the tubesheet flexure load from the expansion load. The net loads were calculated as a function of depth into the tubesheet and compared with the maximum pullout load for 3NODP. The 3NODP load represents the governing criteria for tube-to-tubesheet joint integrity. The tubesheet depth limit occurs when the net contact load exceeds the maximum pullout load.

This section provided a summary of the tubesheet deflection analysis. A more detailed discussion is provided in Section 6.0.

(a,b,c)

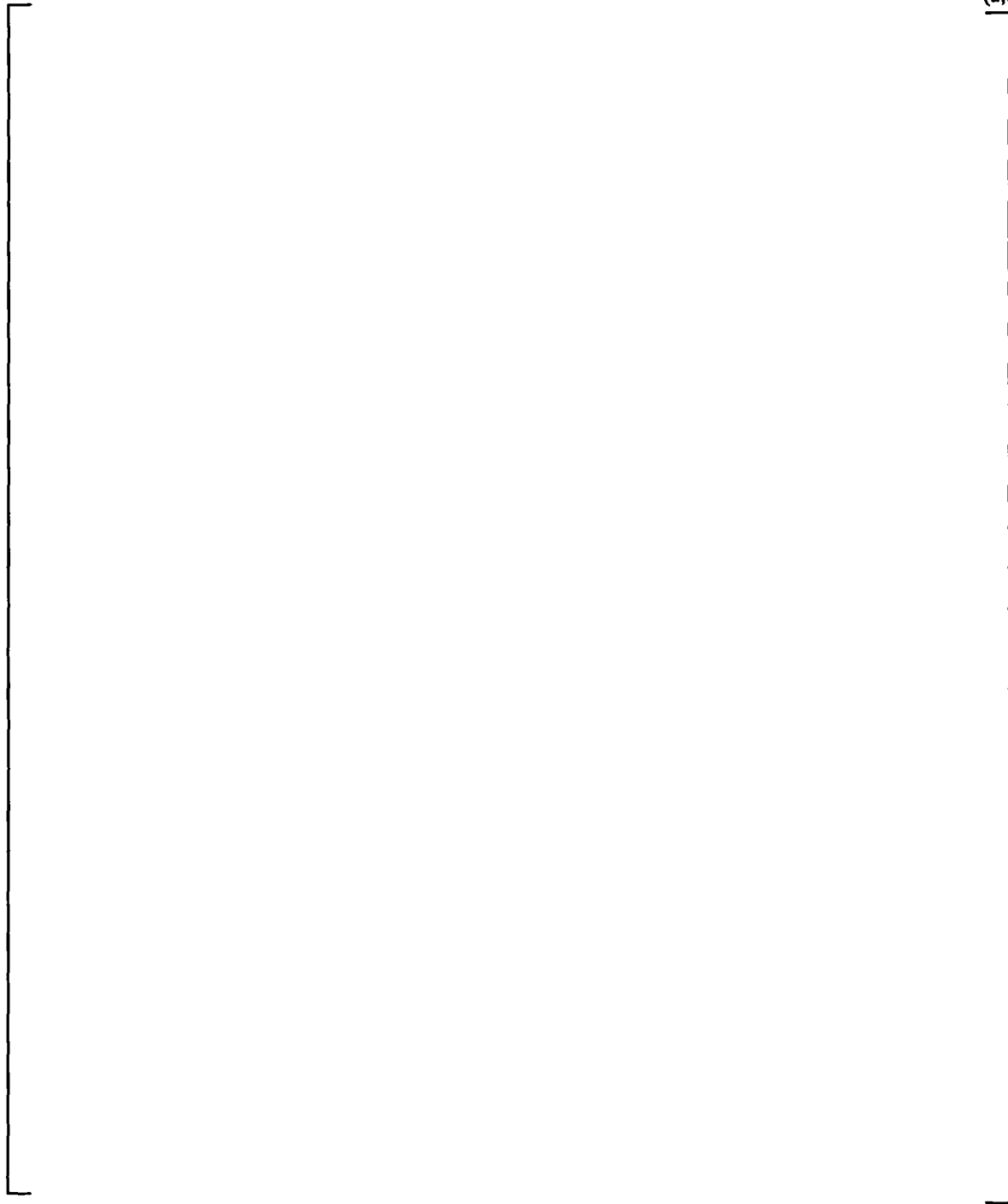


Figure 3-1: Drawing Showing Test Sample Dimensions.



Figure 3-2: Windsor Load Cell Test Controls and Data Plotter

(a,b,c)

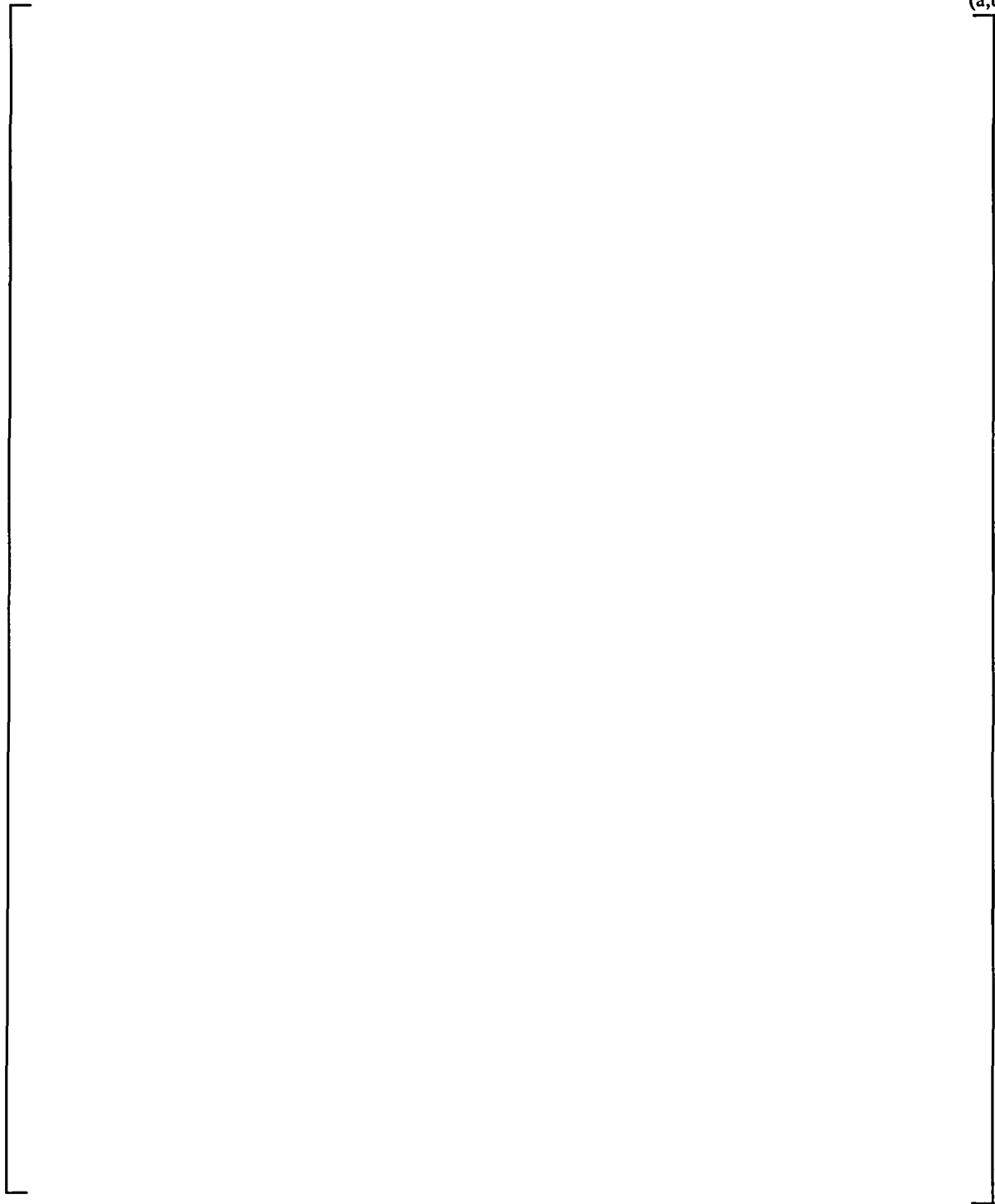


Figure 3-3: Leak Test Equipment Schematic.

4.0 LEAK RATE TESTS AND RESULTS

Analyses documented in Reference 4 demonstrated that the total leakage from the postulated population of degraded tubesheet joints resulted in the bounding criterion for the determination of the C^* inspection length. As described in Section 3.0, additional leak tests were performed to supplement the previous leak rate testing.

The leak rate evaluation for the C^* inspection depth recommendation is based on a combination of empirical and analytical methods. Sections 4.1 and 4.2 describe preliminary and room temperature testing respectively that was performed to establish and validate the methodology for determining the value of C^* based on leak rate. Section 4.3 describes how the limiting faulted temperature was selected. Section 4.4 describes elevated temperature testing. Section 4.5 provides a statistical comparison of the data with the CEOG Task 1154 (Reference 4) data, helping to establish how the data can be used. Section 4.6 and 4.7 provide observations on the effects of temperature, pressure and water chemistry on the leak rate. Section 4.8 provides an evaluation of the leak rate data and a projection of the joint length, i.e., the threshold length for leakage, for acceptable leakage under SLB conditions from through-wall defects located within the tubesheet region.

Leak rate tests were conducted on every joint configuration of every sample. Section 3.2.3 of this report provides details of the testing process; this section provides the results of the testing. Leak tests were conducted after a new joint length had been prepared by cutting a full circumference throughwall notch by EDM and welding new fittings onto the ends of the sample. Each sample was then leak tested at room temperature to visually leak check the fitting welds to assure that a weld leak would not contribute to the measured leakage. Acceptable welds showed no signs of weepage at all after a visual inspection during a five minute (minimum) period at the maximum pressure differential that the sample would be exposed to at elevated temperature. Unacceptable welds were repaired and re-examined.

4.1 PRELIMINARY TESTING

Preliminary leak rate testing was performed to evaluate the test equipment, finalize test procedures and to determine what level of leakage the samples could be expected to have. Sample 1 was prepared in advance of the other samples for performing the preliminary tests. The first EDM notch cut was made at a distance of 3.0 inches below the TTS. A scribe mark was made on the tube at the TTS as a reference point that was used to determine if the tube had moved during the pressurized tests. Fittings were welded to the top and bottom of the sample and leak tests were performed at room temperature. Leakage from the tube-to-tubesheet annulus was observed during the testing as a slowly growing drop of water. The leak rate measurements from the preliminary testing are provided in Appendix A.

Figure 4-1 compares the results of the Sample 1 room temperature leak rate testing with the results of the CEOG Task 1154 leak rates. The Task 1154 data was obtained from Table 5-1 of Reference 4, "Rough Bore Collars: Leak Test Data at Room Temperature." The first leak rate from Sample 1 was comparable to the highest leak rate obtained from Task 1154 (sample 10); the second room temperature leak rate (measured after elevated temperature leak rate testing was completed) was comparable with the remaining Task 1154 rough bore samples. These first set of

tests, comparing similar sets of samples, showed similar leak rates. This suggests that the storage of the samples for a three year period did not have a significant effect on the leak rate characteristics.

Sample 1 at a joint length of 3 inches was also tested at 400°F and 600°F. Appendix B summarizes these results. The system checked out and operated as expected. The tube did not move out of the tubesheet during testing. Various trends were identified in regards to the effect of leak rate on time, temperature and pressure. These are discussed in subsequent sections along with the results from other samples.

4.2 ROOM TEMPERATURE TESTING

All samples were tested at room temperature before testing at elevated temperatures. Most of the samples in this program had measurable leakage at room temperature at pressure differentials of []^(a,b,c) or higher. This leakage was always visible and was seen as a droplet forming on the top of the tubesheet from the tube-tubesheet annulus. Sometimes this droplet formed slowly over a period of several minutes to other cases where the droplet formed rapidly and covered the entire top of the tubesheet collar within a matter of seconds. The leakage was observed to emanate from a few specific locations rather than from the entire annulus evenly.

Appendix A presents a summary of all of the room temperature leak rate tests that were conducted at Westinghouse Windsor and at the STD. The leak rate testing performed at the STD with samples 7 and 37 was performed with several different water chemistries, two pressure differentials and after treatment with secondary side AVT (all volatile treatment) chemistry water. An initial set of tests was performed with deoxygenated deionized water, oxygenated deionized water and simulated primary, i.e., RCS, water. There was no meaningful difference between the observed leak rates from the three different water chemistries.

During a 40 minute test on sample 37, zero leakage was observed at a pressure differential of 1275 psig. Increasing the pressure differential to 2575 psig resulted in a leak rate of []^(a,b,c). After collecting leak rate data for 40 minutes, the pressure differential was dropped to 1500 psig, and no leakage was observed for the entire 10 minute test period (no data was recorded during the 1500 psig run). This was the only leak rate “shut off” observed in this program.

Examination of the initial STD leak rates showed that they were about a fifth of the last comparable leak rates measured in the Windsor facilities. There had been a four month period between the time that the Samples had been tested in Windsor and at STD, during which time the fittings had been cut off of the samples in preparation for bobbin coil testing, and new fittings had been welded on to accommodate the STD facilities. It was judged that there had been significant handling of the samples to allow an oxide to form in the annulus that would partially restrict flow. It was judged that the samples needed to be returned to a baseline oxidation condition. Both samples were subjected to treatment in AVT water for a single []^(a,c) period. When the samples were removed from the AVT water, they were furnace dried and sealed in plastic bags containing desiccant while waiting to be tested further.

After AVT treatment, the samples were tested with RCS water and oxygenated deionized water. The leak rate increased by a factor of two to three from the AVT treatment. The AVT treatment was repeated for an additional []^(a,c) to see if the first treatment had been completed. The samples were then re-tested with RCS water. There was little difference in the leak rates from the second AVT treatment and the first treatment was deemed sufficient.

4.3 SELECTION OF ELEVATED TEST TEMPERATURE

NRC Generic Letter 95-05 (Reference 14), Section 3.b, states that the leak rate methodology described in WCAP-14046 (Reference 15) has been approved by the NRC (Reference 16). Based on the review of the WCAP-14046, it is stated in Table 5-10, "Burst Pressure and Leak Rate Data for 3/4 Inch Tubing", that the SLB leak rates have been adjusted to reference pressure differentials at 616°F. As is noted in Section 4.6 of this report, leak rates were shown to increase as temperatures decreased from 616°F. A test temperature of 600°F was used as a conservative, downward round-off of the approved leak rate temperature.

4.4 ELEVATED TEMPERATURE LEAK RATE TESTING

Elevated temperature testing was performed to characterize the leak rate that could be expected at SLB conditions. As previously noted, the testing did not include pressure induced dilation of the tubesheet holes. A single specimen was first installed into the elevated temperature test vessel, and the entire system was pressurized and visually checked for leaks. All specimens were subsequently heated to the specified test temperature under a nitrogen atmosphere, leak tested and then cooled under a nitrogen atmosphere. All of the elevated temperature testing was performed subsequent to the room temperature leak rate testing. All of the test specimens exhibited measurable leakage at elevated temperature at pressure differentials of []^(a,b,c) and higher. The leak rate tests provided the empirical data for determining the joint length necessary to meet the leakage criteria of 0.1 gpm per steam generator.

Appendix B provides a summary of the elevated temperature leak rates that were observed for each of the specimens in this program. The few tests that had pressures outside of the ±100 psi tolerance or temperatures far from the targeted temperature were considered invalid and are excluded from Appendix B.

There was an effect of time in the leak rate data. Most of the samples started with a relatively high leak rate and did not achieve a steady leak rate for a period of several minutes. The higher leak rate observed during the start of testing is uncharacteristic of leakage that would be observed in an operating steam generator. The data in Appendix B were reviewed to identify those data that had reached steady, or established, values under SLB conditions. Table 4-1 provides a summary of all the established elevated temperature leak rate values. The data in this table consists of valid leak rates (all parameters within specification and close to the targeted parameters), that have demonstrated some degree of an established or steady value. It also provides the basis for the selection of each point. The leak vs. time plots that are mentioned in Table 4-1 can be found in Appendix C. A plot of the SLB condition leak rates as a function of joint length is provided in Figure 4-2.

4.5 STATISTICAL COMPARISON OF C* AND TASK 1154 DATA

An unusual artifact of the Task 1154 data is that all four of its elevated temperature results fall well below the results of all of the C* program data. A statistical review of the results of the different laboratory tests was performed with the goal of determining if the leak rate data from the C* program and the Task 1154 programs could be combined (Reference 17).

The data that were analyzed consisted of paired observations on leak rates and joint length from the C* and Task 1154 programs. The C* and 1154 program sample results were classified according to whether the tube sheet holes were rough bore or smooth bore. The analysis tested whether leak rates for C* and 1154 are different while controlling for the length of flow path and type of hole (rough versus smooth).

The Darcy equation (Reference 18), for flow through porous media, most closely approximates the flow through a tight annular gap:

$$V = \frac{g_c \Delta P}{\alpha \mu L} \quad \text{or, equivalently,} \quad V \cdot L = \frac{g_c \Delta P}{\alpha \mu}$$

where,

- V = average fluid velocity, synonymous with leak rate,
- g_c = 32.174 lb_m·ft/lb_f·sec²,
- ΔP = pressure drop,
- μ = viscosity,
- L = Length of the flow path, and
- α = inverse of the permeability coefficient.

In this analysis, the joint length was assumed to be the only contributor to the leak path. Abstracting from experimental or random variation, the product of leak rate and length of flow path should be a constant if the experiments control for g_c , ΔP , μ , and $1/\alpha$. Hence, the following regression model with binary (“dummy”) variables suggests itself for paired observations on V and L across the C* and 1154 programs,

$$[\quad \quad \quad]^{(a,c,e)}$$

Where:

- b_c, b_0, b_1 = constants of the regression analysis,
- δ_1 = 1 if the observation is from the 1154 program, zero otherwise.
- δ_2 = 1 if the observation is from the “rough” hole category, zero otherwise.
- ε = a regression error term to capture random experimental variation.

And the constant term plus b_0 and b_1 are coefficients to be estimated from the data.

When this model is applied to the C* and 1154 program data, it can be shown that the estimated (ordinary least squares) value of the b_0 coefficient measures the difference between the mean values of $V \cdot L$ for rough and smooth holes, controlling for program, and that the Student’s t

statistic for this coefficient is a test of the hypothesis of no difference in the mean values for V·L between the rough and smooth holes. Similarly, the regression estimate of the coefficient b_1 measures the difference between the mean values of V·L for the 1154 and C* programs, controlling for roughness of holes, and the associated t-statistic is a test of the hypothesis of no difference in the mean values of V·L between the two programs.

The data for the analysis is shown in Table 4-2. The regression results for the model in Equation (1) are in Table 4-3. The estimated coefficient of []^(a,c,e) for δ_1 indicates that the mean value of V·L for the 1154 program is smaller by this amount than the C* program counterpart. The t-statistic for δ_1 of []^(a,c,e) is large enough to indicate (at the 5% level of significance) that this difference would not occur "by chance." Consequently, the null hypothesis of no difference in the two programs is rejected. On the other hand, the t-statistic for the rough dummy indicates that the difference contributed by the roughness measure is small enough to accept the null hypothesis that the rough versus smooth categorization is not a significant differentiator. It is thus dropped from further consideration.

The analysis found that the type of hole is not a statistically significant differentiator and that the mean C* and 1154 leak rates are significantly different. Thus, the Task 1154 and C* samples cannot be combined.

4.6 EFFECT OF TEMPERATURE AND PRESSURE ON LEAK RATE

In addition to the elevated temperature leak rate tests performed at constant temperature, there were four tests conducted on samples where the pressure differential was held steady while the temperature was changed. These tests are listed in Table 4-4.

Figure 4-3 through Figure 4-6 provide plots of the leak rate as a function of temperature for these samples. In all cases there was evidence of hysteresis, showing that changing the temperature affects the leak rate. In all cases, the leak rate decreased with increasing temperature, between []^(a,b,c). Indications are that this trend would continue at higher temperatures. Figure 4-5 and Figure 4-6 suggest that a maximum leak rate is achieved at about []^(a,b,c), and one leg of the hysteresis of Figure 4-4 suggests this as well. This leak rate maximum is not evident in Figure 4-3.

Selected data were ranked and plotted as a cumulative distribution to estimate what the relative effects of temperature and pressure have on the leak rate. Table 4-5 provides the data that was used in this analysis. Figure 4-7 shows a plot of the Table 4-5 data. Using the median as an estimate, the pressure effect is []^(a,b,c) and the temperature effect is []^(a,c,e).

4.7 EFFECT OF WATER CHEMISTRY ON LEAK RATE

The leak test results from this program were considerably higher than the leak rates that were observed in the Task 1154 program for comparable samples and joint lengths. The most significant difference between the Task 1154 program and the C* program was the water chemistry. The Task 1154 program used uncontrolled deionized water that had ample exposure

to air, while the C* program simulated primary water had been deoxygenated and kept under a nitrogen overpressure. A program was conducted to assess the effect of water chemistry by taking Samples 7 and 37 and subjecting them to additional leak rate testing at STD using both deionized water and simulated primary water. Appendix B provides a summary of the leak rate tests performed on Samples 7 and 37. All of the elevated temperature leak rate tests at STD were conducted after the samples had been treated with AVT water. Appendix B shows that both samples had deionized water and primary water leak rates that were roughly the same; in the case of Sample 7, the deionized water produced the slightly higher leak rate; in the case of Sample 37, the simulated primary water produced the slightly higher leak rate. These STD tests demonstrated that a difference in water chemistry (deionized-deoxygenated water and deoxygenated primary water) did not affect leak rate. [

] ^(a,c)

4.8 EVALUATION OF LEAK RATE DATA

The leak rate testing demonstrated, up to SLB pressure, that the largest leak rate was obtained at SLB pressure. It was also demonstrated that 600°F is a conservative temperature to consider in an evaluation of leak rate data. Figure 4-2 provided a plot of the data (from Table 4-1) that had been obtained at 600°F and SLB pressure. In this section, a conservative projection of the joint length that would meet a leak rate criterion of 0.1 gpm per steam generator is provided using the Table 4-1 data.

Figure 4-2 includes a regression line that was calculated by a least-squares fit of the Table 4-1 data. The regression line has a slope of [] ^(a,b,c) and an intercept of [] ^(a,b,c) that can be used to project a joint length that meets a given leak rate criteria. For example, for a leak rate criterion of 0.1 gpm per steam generator in a 10,000 tube steam generator, the leak criterion per tube is $1 \cdot 10^{-5}$. Solving, [

] ^(a,c) However, there are several considerations that have not been accounted for in this basic projection. A correction for the dilation of the tubesheet hole under accident conditions has not been accounted for in this basic projection; this correction is provided in Section 6. NDE positional error has not been added either; this is accounted for in Section 7. The basic projection has not accounted for statistical error of the projection or the interdependency between measurements in this particular data set; these are considered in this section of the report.

In this evaluation, it is assumed that every tube in the generator is flawed below the inspection length. With the entire population of tubes in a generator under consideration, the appropriate bounding case to account for statistical error is based on the confidence interval of the data.

The data in Table 4-1 consists of 21 leak rate measurements obtained from 8 samples. Multiple observations were made on some samples and single observations were made on others. A standard regression analysis on this data set would thus be somewhat erroneous, as some of the observations made on the same sample would already be correlated. This differs from the W*

leak rate analysis where the same number of observations were made on each sample and no single sample had more or less influence on the regression analysis than the other samples.

To account for the interdependency between some of the leak rate measurements, a statistical resampling method was employed to create an artificial population of observations. The method uses resampling with replacement to create the population, and is commonly referred to as bootstrapping (Reference 19).

To generate a bootstrap uncertainty estimate for a given statistic from a set of data, a sub-sample of a size equal to the size of the data set is generated from the data, and the statistic is calculated. This sub-sample is generated with replacement so that any data point can be sampled multiple times or not sampled at all. This process is repeated for many sub-samples, in this case 1000 times. The computed values for the statistic form an estimate of the sampling distribution of the statistic. In this case, the statistic of interest is the confidence interval on the projected joint length at the leakage criteria.

[

$]^{(a,c)}$ Table 4-6 shows the transformed data.

Table 4-7 shows how the sample-with-replacement population is generated. [

$]^{(a,c)}$

After the sample-with-replacement population is generated, there are a total of 1000 sub-samples. [

$]^{(a,c)}$

For each sub-sample, at a given leak rate, Q , the joint length that meets that leak rate can be calculated [$]^{(a,c)}$ The calculation in Table 4-7 projects the joint length, L , from the given leak rate, Q , [

$]^{(a,c)}$

[$]^{(a,c)}$

The result, at a given leak rate, Q , is a total of 1000 joint lengths. As Table 4-7 shows, this can be repeated for any given leak rate. The 1000 joint lengths can then be sorted in ascending order to determine the upper confidence limit.

A one-sided conservative upper $100 \cdot (1 - \alpha)\%$ confidence bound of the sampled population is obtained using the F-distribution to find the smallest value of n such that,

$$\frac{1}{1 + \frac{N - n + 1}{n} F_{1-\alpha, 2(N-n+1), 2n}} \geq P$$

Where N is the total number of simulations performed (in this case $N=1000$) and $P=1 - \alpha$ (Reference 20). To find the 95% upper confidence bound ($\alpha=0.05$) from a total of 1000 sorted simulations, the 962nd lowest value ($n=962$) is used.

Figure 4-2 also includes the 95% upper confidence limit, calculated using the method described above at various leak rates.

The joint length, unadjusted for tubesheet hole dilation and NDE error, that meets leakage criteria for each plant can be calculated using this method. Assuming a leak rate criterion of 0.1 gpm and a given number of tubes per steam generator, the uncorrected joint length that meets the leakage criteria is provided for each plant in Table 4-8. The results are all approximately []^(a,c), with nearly no difference between the largest and smallest steam generators.

Table 4-1: Summary of Elevated Temperature Leak Rate Tests (Continued)

Note	

Table 4-2: Data Used in the Regression Analysis

Established Leak Rate (gal/min)	Joint Length (in)	C* Dummy	1154 Dummy	Rough Dummy	Smooth Dummy
(a,b,c)					

Table 4-3: Regression Results for Equation 2 Model Using C* & 1154 Data

	(a,b,c)
--	---------

Table 4-4: Leak Rate vs. Temperature Tests

Sample	Bore Type	Joint Length (inches)	Average Delta Pressure (psid)	Length of Test (min)	(a,b,c)

Table 4-8: Uncorrected Joint Lengths that the Meet Leakage Criterion for Each Plant

Plant	Assumed Number of Tubes per SG	Assumed SG Leak Criteria at 0.1 gpm/SG (gpm/tube)	Uncorrected Joint Length that Meets Leakage Criteria (inches)
Plant CI	5000	2.00×10^{-5}	6.55
Plant CG	7911	1.26×10^{-5}	6.56
Plant N	8500	1.18×10^{-5}	6.56
Plant CD	9300	1.08×10^{-5}	6.57
Plant CF2	9300	1.08×10^{-5}	6.57
Plant CF3	9300	1.08×10^{-5}	6.57
Plant CE1	10000	1.00×10^{-5}	6.57
Plant CE3	10000	1.00×10^{-5}	6.57



Figure 4-1: Comparison of Sample 1 Room Temperature Leak Test Results with CEOG 1154 (at SLB Pressure).



Figure 4-2: Plot of Leak Rate vs. Joint Length at 600°F, $\Delta P = \text{SLB}$.



Figure 4-3: Sample 2 (Joint Length=1.5") Temperature Dependency.

(a,b,c)



Figure 4-4: Sample 3 (Joint Length=4") Temperature Dependency.



Figure 4-5: Sample 6 (Joint Length=2.25") Temperature Dependency.

(a,b,c)



Figure 4-6: Sample 6 (Joint Length=3", P=NODP) Temperature Dependency.



Figure 4-7: Cumulative Distribution of Temperature and Pressure Effects on Leakage.
(Used to Estimate the Effect on Leak Rate.)

5.0 PULLOUT LOAD TESTS AND RESULTS

In the event that a steam generator tube is circumferentially degraded within the tubesheet, to the extent that separation would occur, meaningful tube axial movement would be expected to be prevented by the tube supports (with or without denting), adjacent tubes in the bend region, and other upper bundle support structure elements. Nevertheless, if a tube separation were to occur within the tubesheet, the portion of the tube from the separation location to the bottom of the expansion transition must withstand appropriate applied loads to meet Reference 2 requirements. An analysis of the vertical constraint provided by the upper bundle elements is provided in Section 7.1 of this report, and is provided as an additional level of conservatism, but is not presented as a primary consideration for pullout restraint. Axial loads must be opposed by the axial restraint provided by the contact pressure between the tube and the tubesheet acting over some interface length.

Reference 4 provided an analysis that showed that the inspection length was limited by the leakage criteria rather than the pullout criteria, thus samples 1-7 were used primarily to develop leak rate data. The completion of a pullout test on a given sample would prevent that sample from being used in any further leak testing. Pullout tests were conducted on every joint configuration except those from samples 36 and 37. Tests were conducted after leak testing on a given joint configuration had been completed. The purpose of this testing was to screen a given joint length to demonstrate that the joint was able to tolerate a 3NODP load. The 3NODP load was not exceeded during these pullout screening tests in order to preserve the sample for possible additional leak rate testing. Section 3.2.2 of this report provided much of the background information for these tests.

This section of the report provides the results of the pullout screening tests. Also, the pullout data from Reference 4 remains applicable to the development of an inspection length and is re-evaluated in this section of the report.

5.1 PULLOUT SCREENING TEST RESULTS

Table 5-1 presents a summary of the pullout screening test results. Rough bore joints as short as []^(a,b,c) were able to withstand the 3NODP load. No smooth bore joint shorter than []^(a,b,c) was shown to withstand the 3NODP load. The sample 3 pullout test at a joint length of []^(a,b,c) was not performed because the sample 4 joint length at 3 inches pulled out under 3NODP conditions, and it was deemed more important to obtain additional leak rate data than to perform this pullout screening.

Sample 1, with a joint length of []^(a,b,c), experienced a tube blowout during room temperature leak rate testing at a pressure of []^(a,b,c) which is well below the lengths discussed in Section 6. As Section 3.2.2 of this report explained, this event prompted the change in the applied internal pressure during pullout screening. Smooth bore samples 3 and 4 did not withstand the 3NODP load at joint lengths of []^(a,b,c), respectively.

Table 5-1 also presents the calculated pullout force with the end cap load added to the external tensile load. The end cap load is calculated by multiplying the internal pressure by the nominal tubesheet hole diameter (0.758 inch).

These pullout forces are consistent with the pullout forces measured in the CEOG Task 1154 program, as is noted below.

5.2 TASK 1154 PULLOUT TESTS

This section provides a brief summary of the CEOG Task 1154 pullout test program (Reference 4). In CEOG Task 1154, pullout tests were conducted on three sample sources:

- A seven tube to tubesheet joint (Ringhals) mockup
- The Boston Edison canceled plant as-built steam generator
- Tube to tubesheet joint mockups (collars)

In each case, the steam generator tubes were cut at measured distances below the “top of the tubesheet.” All tests were conducted as a function of joint length that is nominally the length of the tube from the TTS to the cut surface.

Seven-Tube (Ringhals RSG) Tubesheet

In the mid-1980s, a tube to tubesheet joint mockup was fabricated as a demonstration for a potential RSG project for the Ringhals plant in Sweden. The tubesheet was bored on a lathe and that the BTA process was most likely simulated. The tubesheet was the standard Class 508 carbon steel material but was only 8 inches thick. Alloy 690 tubing with a 0.75” OD and a 43 mil wall thickness was expanded into the tubesheet by the standard CE process including the positioning roll and seal weld. Pullout testing of Alloy 690 compares favorably to Alloy 600 because the material property specifications are the same.

Boston Edison Steam Generator

The Boston Edison steam generator was fabricated for the Boston Edison NSSF contract that was subsequently cancelled. The lower portion of one of the steam generators had been preserved as a test bed. As such, the tube to tubesheet joints represented a set of as-built conditions typifying the manufacturing processes of the vintage of most CEOG operating steam generators and so were the most representative of the results that was expected from CEOG steam generators. The tubesheet material was typical of operating units; the tube holes were also typical in terms of size, tolerances and surface finish of a rough bore finish (gun-drilled) in terms of the surface finish test conditions. The tube material was typical of production material installed in several CE designed steam generators (provided by Noranda, 0.042 inch average wall thickness) and had the normal variations in tube wall thickness and yield strengths that would be expected in operating units. The explosive expansion process was also obviously typical of the techniques employed for CE steam generators.

Tube to tubesheet joint mockups

The tube to tubesheet joint mockups used in the CEOG Task 1154 pullout tests were identical to those used in the C* leak test program.

Pullout Load Tests Methods

Pullout testing was conducted in laboratory facilities in Chattanooga, Tennessee and in Windsor, Connecticut using calibrated load cells. The equipment for the pull tests in the Chattanooga and Windsor laboratories were similar and both were calibrated to accepted standards. For the tests performed in Chattanooga, a mechanical gripper secured the upper end of the tube to the load cell. A tight fitting mandrel inside the tube prevented the gripper from deforming the tube at the gripper location and a bracket secured the mockups to the piston that applied the load. For the tests performed in Windsor, a retention plate with a threaded hole was used to secure the upper end of the tube to the load cell and a similar plate was used to secure the collar to the crosshead. Threaded plugs that had a means of allowing water to enter and exit the tube were welded to the upper end of the tube and to the lower end of the collar. The threaded portion of the plugs was screwed into the threaded hole of the two retention plates. X-Y plotters were used to record load versus crosshead displacement. After the specimen was secure in the test machine, loads were applied at a fixed crosshead displacement rate in the Windsor tests and at a manually adjusted load in the Chattanooga tests until the severed tube was pulled from the tubesheet. The load at which first slippage of the tube in the tubesheet occurred and the maximum load during the test were noted and recorded. A plot of load versus crosshead displacement was also obtained for each mockup tested. In the Chattanooga tests, the slope of the ascending load vs. time curve varied as the rate at which the hydraulic pump pressure regulator screw was adjusted. This was done manually and intentionally slowly so as not to miss the data readings. Once the tube began to move, the pressure regulator was not adjusted any more, unless the tube stopped moving. In most cases, the maximum force was achieved after the tubes had moved some distance.

The Chattanooga load cell applied a manually adjustable constant load process. The Windsor load cell was applied in a constant displacement rate process. The test plan called for two collar specimens to be tested in Chattanooga as a cross-reference between the Chattanooga and Windsor load cell tests to show that the test setups would provide comparable results. The difference in processes results in some variability in the results as indicated by the two rough bore collar specimens (specimens 20 and 21) tested in Chattanooga and the remainder of the rough bore collar specimens tested in Windsor. Specimens 20 and 21 were made up of tubes with wall thicknesses of 42 mils. Whereas, all other rough bore samples were made up of 48 mil wall thickness tubes. The difference in wall thickness was judged to have little significance as a contributor to the variation in the resulting maximum pullout loads; the difference in cross-sectional areas is only about 12% and other factors (surface roughness variations, sample preparation variations, testing technique, etc.) were considered to have greater significance.

5.3 ANALYSIS OF PULLOUT TEST RESULTS

Table B.1-1 of Reference 22 provides a summary of rough bore pullout test data obtained from the Boston Edison steam generators and the Task 1154 laboratory data. Table 5-2 provides a

compilation of the Reference 22 (Table B.1-1) pullout data that was obtained at room temperature and with no internal pressure. Reference 22 (Table B.1-1) only provides the targeted joint length for the Task 1154 data; the actual joint length for this same set of data is found in Table 4-3 of Reference 4. None of the samples listed in Table 5-2 were previously leak tested at an elevated temperature.

The data in Table 5-2 was scaled to account for differences in tube wall thickness and differences in testing procedures. This wall thickness and process adjustment is described in Reference 22 as follows:

The pull data is adjusted for two overall effects: (1) the Plant CF steam generator tubes are 48 mil wall so the 42 mil wall data has been scaled to 48 mils; and (2) the pull tests conducted at the Windsor location was adjusted down to the Chattanooga data to account for process variability (and material properties). The mean yield strengths of the 48 mil tubes are approximately 9 ksi greater than the 42 mil data. The assumed mean yield of the Boston Edison tubes at 45 ksi is the mid-point of the standard CE design specification. The test specimens had a yield strength at 54 ksi. The effects of the yield and process differences are not separable and are considered in combination. It is noted that a process difference is evident because the difference between the tests conducted at the two locations is larger than can be accounted for in tube yield strength differences. The adjustment for item (2) was conservatively applied by [

] ^(a,c)

Figure 5-1 provides a plot of the 48 mil wall rough bore data. In Figure 5-2, the pull data that occurs above the yield point of the tubing (54 ksi) is plotted, but not used to determine the lower confidence bound. The sample 1 blowout data is shown to be consistent with the rest of the pullout data, however this pressurized pullout data is not used in the regression analysis either. The regression analysis is used in the determination of the effect of tubesheet hole dilation in Section 6. The Section 6 analysis requires a determination of the contact pressure due to the expansion process alone, which is derived from the slope of the regression line in Figure 5-1.

Figure 5-2 presents a similar plot for the 42 mil wall rough bore data.

Table 5-3 presents a summary of smooth bore pullout data from the Task 1154 program and includes the Ringhals data from the Reference 4 report. Pullout tests conducted at an elevated temperature or with an internal pressure have been excluded because the Section 6 tubesheet hole dilation requires the contact force from the expansion process alone. Figure 5-3 shows a plot of the Task 1154 and Ringhals smooth bore pullout data and includes Samples 3 and 4 for comparison. As with the rough bore plots, the pullout screening tests are provided for comparison but are not included in the regression analysis. Nevertheless, the pullout screening test data are consistent with the other smooth bore pullout data.



Figure 5-1: Pullout Force for 48 mil Wall Rough Bore Samples from the Boston Edison Steam Generators, CEOG Task 1154 and Sample 1.

(The tests that used tubes with 42 mil data were scaled to 48 mil wall. Process adjustment made to Task 1154 data).



Figure 5-2: Pullout Force for 42 mil Wall Rough Bore Samples from the Boston Edison Steam Generators and CEOG Task 1154.
(The tests that used tubes with 48 mil data were scaled to 42 mil wall. Process adjustment made to Task 1154 data).



Figure 5-3: Pullout Force for 42 mil Wall Smooth Bore Samples from CEOG Task 1154, Ringhals Samples and Samples 3 and 4.

6.0 TUBESHEET DEFLECTION ANALYSIS

Tubesheet deflection under primary to secondary differential pressure causes a dilation of the tubesheet holes in the upper half of the tubesheet that is a maximum at the secondary face, i.e., top of the tubesheet. The dilation diminishes to zero at the tubesheet neutral plane, which is near the mid-plane, and contracts below the neutral plane. The hole dilation causes a reduction in the contact forces holding a tube in the tubesheet and reduces the resistance to any leakage if throughwall flaws exist.

6.1 FINITE ELEMENT MODEL ANALYSIS

The effect of tubesheet deflection (flexure) on the contact load between the tube and tubesheet was modeled using Finite Element Model (FEM) analysis (Reference 23). The FEM analysis provided a direct output of the tube-to-tubesheet interface loads, which included the reduction of the contact loads from the pressure and thermal expansion and the tube expansion residual pressure in the upper part of the tubesheet.

Tubesheet dilation effects applied to a single tube FEM were calculated from the tubesheet stresses for the worst case loading conditions documented in the respective CE steam generator design reports. Symmetry of the tube/tubesheet was used to reduce the finite element model size, incorporating axisymmetric 2-D modeling of the tube and tubesheet. The model length was 8.0 inches from the tubesheet secondary face (TTS) into the tubesheet. Because the results are linear with tubesheet axial position, lengths greater than 8 inches can be linearly extrapolated.

For the FEM analysis the internal tube pressure was set to 0 psia for the flexure case only with the thermal for the tube and tubesheet at 600°F. The tube hole displacements applied to the model were based on an equivalent solid plate effect (which considers the tube hole sizes and pattern) as documented in the respective CE steam generator design reports. In these design reports, a conservative classical interaction type of analysis was performed on the tubesheet including the primary head, secondary shell, and stay cylinder in the interaction model. The divider plate, which would reduce deflections, is conservatively neglected. The worst location (point of maximum tubesheet deflection) in this interaction model from the design reports was used in the FEM. The pressure differential at this location resulted in the maximum equivalent solid plate stresses and maximum tube hole displacements to use for input into the FEM. The tubesheet membrane and bending stresses as a function of depth are applied to the FEM to determine the loss of contact pressure due to this loading. Based on an evaluation of the original design reports, the Plant CI tubesheet flexure stresses were determined to be []^(a,c) than the stresses from the Plant CF evaluation (Plant CI does not have a stay cylinder) so the Plant CI values for dilation loads were scaled up from Plant CF/Plant CD results.

The following bounding conditions were considered in the finite element analysis (FEA):

[

$$J^{(a,c)}$$

6.2 DILATION CORRECTION FOR BURST

Burst criteria in NEI 97-06 are defined by the maximum of three times the NODP or 1.4 times the differential pressure associated with the most severe accident. The 3NODP criterion governs for all CE SG designs. The 3NODP tests conducted in the C* test program and the CEOG Task 1154 testing did not directly account for tubesheet dilation, rather the dilation was determined analytically in the FEM analysis described above and applied as described in this section. The NEI 97-06 and EPRI requirements do not require the combination of tubesheet bending at SLB conditions with the 3NODP burst criteria, but these criteria were conservatively combined in this analysis.

The normal operating pressure differential pressure for the Plant CF 2 & 3, Plant N, Plant CD, Plant CG, and Plant CE1 & 3 steam generators are shown in Table 6-1. Also included in this table is three times the Normal Operating Pressure (NOP) differential. The inner radius of the tubesheet hole in the non-expanded region is [$J^{(a,c)}$], which results in an inner tubesheet hole area of [$J^{(a,c)}$]. Thus, the maximum pullout load would be three times NOP times [$J^{(a,c)}$].

The following points were used in the correction for dilation:

- The results from the tube Pullout Tests for the tubesheet collars at room temperature documented in Section 5 of this report were used to establish the residual contact load from the tube expansion. For example, the slope of the bounding regression line illustrated in Figure 5-1 represents the force per unit length, i.e., [$J^{(a,c)}$] for the 48 mil tubing in a rough bore tubesheet hole.
- A coefficient of friction of [$J^{(a,c)}$] was used based on similar applications (References 24; 25) to determine the axial load due to the hole dilation from the normal load calculated in the FEM analysis. The load due to dilation is a negative number in the upper tubesheet region indicating a reduction in load in the tube to tubesheet joint.
- The net axial contact load results from combining the tubesheet flexure load and the expansion load. The net loads were calculated as function of depth into the tubesheet and compared with the maximum pullout load for three times the Normal Operating Differential Pressure (NODP). The three times NODP represents the governing criteria for tube/tubesheet joint integrity based on the guidelines specified in NEI 97-06. Three times NODP exceeds the differential pressure effect for the main steam line break (MSLB) for all CE designed steam generators. The tubesheet depth where the net contact load exceeds the 3NODP pullout load is the joint length that ensures that the burst criteria are met.

The pullout loads provided in the plots of pullout force versus joint length for 48 and 42 mil tube wall thicknesses in section 5 are equivalent to the end cap loads that would act to force the tube from the tubesheet. If these axial forces are greater than the pullout loads provided in Table 6-1 for a given joint length then the joint satisfies the burst criteria. The correction for tubesheet hole dilation reduces the joint contact force by an amount determined in the FEM analysis. The contact force and the dilation force acting normally on the tube wall are converted to axial forces by multiplying by the coefficient of friction. The tubesheet deflection (flexure) loads in the X and Z (F_x and F_z) directions with respect to the depth of the tubesheet from the secondary face are illustrated in Table 6-2 through Table 6-7. The summation of the axial loads provided in the following tables is compared to the pullout loads in Table 6-1. The burst based inspection lengths for each plant are provided in Table 6-8.

The results provided in Table 6-2 through Table 6-7 are summarized in Table 6-8. The pullout load criteria are met at depths ranging from 2.25 – 4.25 inches from the secondary face of the tubesheet. As indicated in Table 6-8, a []^(a,c,e) adjustment for NDE probe location uncertainty is added to each pullout result.

6.3 DILATION CORRECTION FOR LEAKAGE

The burst based inspection length is bounded by the leakage based inspection length for all CE designed steam generators. The leak test results provided in Section 4 require adjustment to account for tubesheet hole dilation. Hole dilation reduces the contact force and thereby the resistance to leakage. The method for the dilation correction and the results are provided in this section. The leak limit is established for the limiting design basis accident which for CE design units is the MSLB. The flexure for the tubesheet and the resultant tube hole dilation are determined at MSLB conditions.

The net radial contact pressure of the combined effect of expansion, MSLB pressure and temperature, and tubesheet flexure results in no gap between the tube and tubesheet at any location. The absence of a gap indicates that the leakage would be significantly restricted despite any tubesheet flexure. Additional compression will result from the tube pressure and to a lesser extent thermal expansion. The tube to tubesheet stress considering the expansion of the tubesheet hole due to a MSLB pressure of 2560 psi is []^(a,c) compression for the 0.048" tube wall thickness and []^(a,c) compression for the 0.042" tube wall thickness based on the exact formulae for thick-walled cylinders, e.g., tubesheet simulant, in Reference 26. If it is postulated that the reduction in contact force is inversely proportional to the flow restriction (characterized as the tube-to-tubesheet diameter difference), then the length of the flow region must be increased by that proportion to achieve the same leak rate. The contact force is directly proportional to the axial load. Therefore, in order to compute the ratio of the total contact due to expansion, pressure, temperature and tubesheet bending to the contact due only to expansion pressure and temperature, a sum of the forces method described below was used.

A sum of the forces method is used as part of the determination of the equivalent length in the leak vs. length results provided in Section 4. The sum of the forces at any elevation z, F_z , is the

sum of the contact force; the force due to dilation; the force due to pressure; and the force due to temperature. The dilation force is negative in value.

$$\Sigma F_z = F_c + F_d + F_p + F_t$$

Where:

F_c = joint contact force (slope of the 95% bound line in Figures 5-1, 2, 3).

F_d = force accounting for tubesheet hole dilation (Reference 23).

F_p = force from RCS pressure at MSLB differential pressure.

F_t = force from the differential thermal expansion of materials.

The summation of forces and the relation to the joint length are tabulated in Table 6-9 through Table 6-14 and summarized in Table 6-15 for the respective CE designed steam generators. The columns in these tables are defined as follows:

Depth in Tubesheet

This column in each table is the length of the joint or the axial position z in the tubesheet in the dilated tubesheet hole. The []^(a,c) increments correspond to the tubesheet deflection analysis (Reference 23) increments. The length listed in this column is that length which corresponds to the "Cum No-Dilate Length" equal to (or just greater than) the non-dilated joint length that meets the leakage criteria. It is the recommended inspection length without NDE correction at the leak rate criteria assuming all tubes are severed.

TS Joint Axial Force (F_c)

F_c is the contact axial force due to the expansion at each incremental elevation or joint length from Figures 5-1, 2, 3 in Section 5. The joint contact force varies according to tube wall thickness and tubesheet hole surface roughness. Note in the Figures 5-1, 2, 3 that for the 95% bound line the extreme values for a small fraction (5%) of tubes are conservatively assumed to have no contact pressure to a joint length up to approximately one inch.

RCS Pressure and Diff. Thermal Axial Force ($F_p + F_t$)

The RCS Pressure and Diff. Thermal Axial Force is the force due to RCS pressure inside the tube plus the force due to the differential thermal expansion between the tube and tubesheet at 600° F. The force is equal ([]^(a,c)) for both 42 and 48 mil wall tubing because of the compensating effects on force in the internal pressure and differential thermal expansion.

Initial Axial Force ($F_c + F_p + F_t$)

The initial axial force is the sum of the TS Joint Axial Force, the RCS Pressure, and Diff. Thermal Axial Force.

Dilation Axial Force (F_d)

F_d is the axial force due to dilation which is the reduction of force due to tubesheet flexure from Reference 23. The axial force due to dilation to a depth of 8.0 inches is calculated from the computer files in Reference 23. For the increment lengths from 8 inches to 16 inches into the tubesheet, the average delta in the axial force due to dilation for the first 8 inches is extrapolated and conservatively applied to the next 8 inches into the tubesheet. This force is a negative value (tensile force) down to approximately the mid-plane of the tubesheet after which it is a positive value (compressive force).

Net Axial Force ($F_c + F_p + F_t + F_d$)

The net axial force is the sum of $F_c + F_p + F_t + F_d$

Net/Initial Ratio ($F_c + F_p + F_t + F_d$) / ($F_c + F_p + F_t$)

The ratio of the sum of all forces to the sum of the forces without dilation is the fraction of the contact force at MSLB compared to the “unbent” tubesheet condition.

Equivalent No-Dilate Length (Net/Initial Ratio x []^(a,c))

This is the joint length in the “unbent” tubesheet corresponding to the equivalent “depth in tubesheet” []^(a,c) increment joint length from the first column for the tubesheet at MSLB conditions.

Cumulative No-Dilate Length

The cumulative non-dilated joint length can be indexed to the results from the leak rate tests. The joint length at the leak rate criterion of 0.1 gpm (from Table 4-8) is indexed in this column to the equivalent joint length for MSLB conditions in the “Depth in Tubesheet” column. Linear interpolation of the appropriate results in Table 6-9 through Table 6-14, indicated by bold type, produces the recommended inspection length for each plant or class of plants, excluding NDE probe positional error. Table 6-15 summarizes the corrected results with and without the addition of the []^(a,c,e) NDE probe location uncertainty. The leak-based values bound the burst-based values from Table 6-8 and are used as the recommended inspection length.

Table 6-1 : Required Pullout Load for 3NODP

Plant	Primary Pressure (psig)	Secondary Pressure (psig)	Differential Pressure (psid)	3NODP (psid)	Required Pullout Load (lbf)	(a,b,c)

Table 6-8: Burst Based Inspection Length
Including Tubesheet Deflection and NDE Corrections
For All CE Designed Steam Generators

Plant	Burst Based Inspection Length Corrected for Dilation (inches)	Burst Based Inspection Length Corrected for Dilation and NDE (inches)
Plant CI	2.75	3.1
Plant N	2.25	2.6
Plant CF/Plant CD	2.25	2.6
Plant CG	4.25	4.6
Plant CE1	2.50	2.8
Plant CE3	4.00	4.3

Table 6-15: Inspection Length Based on Leakage

Plant	From Table 6-8: Burst Based Inspection Length Corrected for Dilation and NDE (in.)	From Table 4-8: Uncorrected Joint Length that Meets Leakage Criteria (inches)	Interpolated Leak Rate Based Inspection Length Corrected for Dilation (in.)	Leak Rate Based Inspection Length Corrected for Dilation and NDE (in.)
Plant CI	3.1	6.55	11.1	11.4
Plant N	2.6	6.56	9.8	10.1
Plant CF/Plant CD	2.6	6.57	10.1	10.4
Plant CG	4.6	6.56	11.3	11.6
Plant CE1	2.8	6.57	10.1	10.4
Plant CE3	4.3	6.57	11.3	11.6

7.0 OTHER FACTORS

There are several miscellaneous factors that can also be considered regarding the conservatism in establishing the criterion. Among these are the role of the upper bundle structure (Section 7.1), the effect of the EDM cuts on the laboratory leak rates (Section 7.2), the presence (or lack) of an expansion taper as is present with WEXTEx expansions (Section 7.3), NDE axial position uncertainty (Section 7.4), and a possible method to characterize the tubesheet hole surface roughness with NDE (Section 7.5).

7.1 VERTICAL CONSTRAINT EVALUATION

7.1.1 Summary

A defense in depth portion of the justification for partial-length RPC inspection of the tube joint includes the constraint provided by the upper bundle structural elements. This constraint would limit the vertical motion that would ensue if the tube potentially separated within the tubesheet due to circumferential cracking or other forms of degradation (such as IGSCC initiated cracks).

A stack up of tolerances was developed to show how the tube vertical constraint mechanically limits the pullout joint length. This was conducted on a bounding plant basis. The support systems on the secondary side of the steam generator were considered for the tube bundle and individual tubes, which consist of tubes with 90° bends and horizontal runs between the bends, and tubes with U-bends.

The tubes with horizontal runs are supported by a vertical and horizontal support system that supports the weight of each tube and would additionally provide restraint against vertical movement for each tube in the case of a severed tube event. The CE-designed steam generator has a robust tube support structure unique to the CE design. The tubes are supported laterally by two diagonal bars (batwings) and up to seven vertical grids anchored near the top of the tube bundle shroud. The interlocked tube bundle support structures (vertical grids) are connected by welding to I-beams that are welded to the tube bundle shroud. This structure cages internal tubes and would limit axial movement of a tube end that was severed and free to move within the tubesheet.

Figures 7-1 through 7-4 provide selected schematics and photographs depicting the installed tubes with their vertical and horizontal supports. These schematics and photos provide a general picture of how the tubes interact with the support system.

7.1.2 Vertical Constraint Determination for Plant CI, Plant CE and Plant CG

The steam generator tube bundle consists of:

- Tubes with low row numbers (Rows 1 through 18), with U-bends, and

- Tubes with high row numbers (Rows 19 through 103 for Plant CI, through 138 for Plant CG, and through 159 for Plant CE), with 10-inch radius 90° bends and horizontal runs between the bends.

The low row U-bend tubes do not require support in the horizontal direction because they are laterally supported by the eggcrate tube supports and are relatively short. The longer tubes are supported by up to seven vertical grids (depending on location) that support the weight of each tube and will provide restraint against vertical movement in the case of a severed tube event. Plant CI, Plant CE3 and Plant CG (RSGs) steam generator drawings were reviewed to determine the maximum clearance between the tube and the adjacent support components (above and below each tube). The maximum clearance is []^(a,c) including consideration for the tolerance range on material thickness and the width of support openings.

The upper support assembly consists of a welded grid with openings which capture each tube. This grid is attached to the upper support structure by welding and bolting. The upper support structure is welded to the steam generator baffle assembly. Individual tubes are captured in such a manner that vertical movement is prevented by the supports or neighboring tubes at the next higher elevation.

The tubes in rows 26 through the largest row number are coupled by vertical grid supports. The tube bundle and supports expand vertically (thermal growth) as a unit. The longer tubes in the tube bundle expand more than the shorter tubes according to their length. Since the tubes are connected through the support grid, thermal stresses develop in each tube at operating temperature. These tubes assume a deflected shape during operation which would further restrict any vertical movement of the individual tube.

The outer row tubes extend beyond the last vertical grid. The center of the vertical length of tubes in the last outer row would react through a cantilever distance in the event of a tube sever. These tubes can deflect by the primary and secondary system differential pressure end cap load acting on a severed tube; any tube on the periphery of the bundle could move vertically far enough to be removed from the tubesheet. The outer tube in each row or line would be considered at a peripheral location which includes the last two rows of tubes (for Plant CI the last two rows are 102 and 103; for Plant CG the last two rows are 137 and 138; and for Plant CE the last two rows are 158 and 159).

Tubes located inside the peripheral tubes but within the vertical grid system (Rows 26 through and including two row numbers less than the highest row number) can also move vertically. However movement is restricted to the distance vertically up to the neighboring tube (nominally 1.0 inch except for Plant CI which can move 0.5 inch). Once the postulated severed tube reaches the tube above it, the movement is restricted by the support grid system and all other tubes connected to the vertical grid. Hence, all tubes except those located on the periphery, will be limited to a nominal one-inch movement (0.5 inch for Plant CI) in the vertical direction.

Tubes located outside the vertical grid system but not on the periphery may be capable of moving up to []^(a,c) In this case the tube above the severed tube is not supported by the vertical grid and may be moved out of the way. However, once the severed tube “squeezes”

between two intact tubes its horizontal movement is limited and it would be captured by tubes in the next higher tube row. Therefore the maximum vertical distance any tube other than peripheral tubes can move is limited to approximately []^(a,c) (for tubes in Rows 1 through 25). There is no restriction of movement for the peripheral tubes.

7.1.3 Vertical Constraint Determination for Plant CF, Plant CD and Plant N

The designs of the Plant CF steam generators were reviewed and are representative of the Plant CD and Plant N steam generators. The steam generator tube bundle tubes consist of:

- Low row number tubes (Rows 1 through 18) with U-bends, and
- Higher row number tubes (Rows 19 through 147) with 90° bends and horizontal runs between the bends.

The low row U-bend tubes do not require support in the horizontal direction because they are close to an eggcrate and are relatively short. The longer tubes are supported by up to seven vertical grids (depending on location) that support the weight of each tube and provide restraint against vertical movement in the case of a severed tube event. Plant CF, Units 2 & 3, steam generator drawings were reviewed to determine the maximum clearance between the tube and the adjacent support components (above and below each tube). The clearance is []^(a,c) including consideration for the tolerance range on material thickness and the width of slots.

The upper support assembly consists of a welded grid with openings which capture each tube. This grid is attached to the upper support structure by welding and bolting. The upper support structure is welded to the steam generator baffle assembly. Individual tubes are captured in such a manner that vertical movement is prevented by the supports or neighboring tubes at the next higher elevation.

The tubes in rows 26 through 147 are coupled by vertical grid supports. The tube bundle and supports expand vertically (thermal growth) as a unit. The longer tubes in the tube bundle expand more than the shorter tubes according to their length. Since the tubes are connected through the support grid, thermal stresses develop in each tube at operating temperature. These tubes assume a deflected shape during operation which would further restrict any vertical movement of the individual tube.

The maximum distance between the last vertical grid and the center of the vertical length of tubes in Row 147 is []^(a,c) These tubes can deflect by the primary and secondary system differential pressure end cap load acting on a severed tube. In fact, any tube on the periphery of the bundle could move vertically far enough to be removed from the tubesheet. The outer tube in each line would be considered at a peripheral location (total of 175 tubes, which includes all of Rows 146 and 147).

Tubes located inside the peripheral tubes but within the vertical grid system (Rows 26 through 145) can also move vertically. However, movement is restricted to the distance vertically up to

the neighboring tube (nominally []^(a,c)). Once the severed tube reaches the tube above it, the movement is restricted by the support grid system and all other tubes connected to the vertical grid. Hence, all tubes in rows 26 through 145 (except those located on the periphery), will be limited to a nominal one-inch movement in the vertical direction.

Tubes located outside the vertical grid system (Rows 1 through 24) but not on the periphery may be capable of moving up to []^(a,c). In this case the tube above the severed tube is not supported by the vertical grid and may be moved out of the way. However, once the severed tube "squeezes" between two intact tubes its horizontal movement is limited and it would be captured by tubes in the next higher tube row. Therefore, the maximum vertical distance any tube other than peripheral tubes can move is limited to approximately []^(a,c) (for tubes in Rows 1 through 25) or []^(a,c) (for Rows 25 through 145). There is no restriction of movement for the peripheral tubes (total of 175).

7.2 EDM CUTTING EFFECTS

EDM cutting generates mild heat in the cut area. There was a concern that the cutting process would obstruct the leakage path. To determine the effects of the EDM cutting process, an Alloy 600 tube was rolled into a tubesheet collar, and a cut was made using the same process that was used to make the EDM cuts in the leak test samples. This sample was then sectioned axially, mounted in epoxy and polished to a mirror finish using silicon carbide papers and diamond particle solutions.

Figure 7-5 provides the results of this metallography. The figure shows two different magnifications of the same area. The photos show the tube wall in a longitudinal cross section, and the thicker tubesheet collar. The tubesheet and tube are separated by a narrow annular gap. The cut is slightly wider than the 40 mil wide electrode that was used to make the cut near the inner surface of the tube. The cut penetrates through the tube wall completely and goes into the tubesheet wall slightly.

There is no evidence whatsoever of the cut causing blockage of the narrow annulus between the tube and the tubesheet. The annular gap remains relatively constant along the entire length of the sample, even in the vicinity of the cut. There is also no evidence of the tube pulling away from the tubesheet in the vicinity of the cut.

7.3 EXPANSION TAPER

Microscopic examination of tubes and tubesheet collars removed after pullout testing indicate that a taper is very small to non-existent. It is reasonable to expect that a taper would not result because of the process design and controls. A review of the CE-designed joint process (Reference 4) showed that the plastic charge carrier of the expansion charge extended beyond the secondary face of the tubesheet. The plastic served two purposes: (1) to hold the position of the primer cord and (2) to carry the explosive force uniformly through the range of the tubesheet. The explosive force carry function apparently is effective in providing a distinct transition from the expanded to non-expanded tube diameter and negating any reduction in contact at or just below the bottom of the transition, i.e., taper. The review of the CE-designed joint process

described in Reference 4 indicated that any taper in the charge assembly plastic carrier was considered a defect and was rejected. NDE measurements of tubesheet joints do not indicate the presence of a taper in operating units or in the test mockups.

7.4 NDE AXIAL POSITION UNCERTAINTY

The W* (Reference 24) NDE measurement uncertainties were reviewed for applicability to the CE-designed steam generators. Model 51 steam generators have 0.875 inch OD, 50 mil wall thick tubes that are explosively expanded into the tubesheet. The EPRI database for NDE techniques provides a qualified technique for the +Point probe detection of flaws in expansion transitions which has been qualified for both Model 51 and CE design steam generator tubes. By extension, based on the fact that the +Point capability is better away from the transition because of reduced probability of probe shoe lift-off, the NDE uncertainties developed for the W* region below the top of the tubesheet are taken here as equivalent for CE-designed units.

NDE Uncertainties for Inspection Distance Measurement

NDE uncertainties were developed for the required inspection distance using test specimen and NDE analysis results for WEXTEx expansions reported in Reference 24. The data in this report were reanalyzed to obtain the NDE length uncertainties associated with the distance between the bottom of the expansion transition (BET) and an axial crack tip or circumferential crack located more than 5 inches below the top of the tubesheet. The NDE sample configurations, NDE data acquisition and analysis and the resulting NDE uncertainties are described below.

NDE Sample Configurations

To provide the “ground truth” for the determination of the NDE uncertainties, four single-tube and five tubes from a 21-tube mockup with explosively expanded tubesheet joints were prepared with 50% throughwall, ID-originated EDM notches of varying lengths, inclination angles, and elevations relative to the top of the simulated tubesheet collar and the BET. The “ground truth” is taken as the actual value or true value for the flaw size upon which the NDE measurement is compared. Single-tube samples (NDE-01-1, NDE-01-2, and NDE-02-1 in Table 7-1) were machined with axial EDM notches positioned at various elevations. The axial flaws on an individual sample were all of the same length, as were the inclined flaws on NDE-01-2 and NDE-02-1. For sample NDE-02-2, all the axial flaws were nominally 1.0 inches long and had no intentional inclination, but their spacing was varied to obtain a sense of the resolving power of three rotating coil configurations. Five samples designated TVA-10, 11, 12, 19, and 20 were part of a 21 tube, explosively expanded tubesheet mockup which contained axial notches of different lengths positioned at various elevations relative to the top of the tubesheet.

The position of the BET was determined for each sample. This was performed by measurements of the ID of the samples at different positions around the tube ID with an indicator (single tube mockups) to find the unexpanded elevation of the transition. For the single tube samples, an average of BET elevation measurements made at 45° intervals is applied to define the reference BET position for the NDE uncertainties. For the TVA samples, two measurements were made of the distance from the top of the tube to the tubesheet and to the BET. An average of the two

measurements is used to define the BET positions for the TVA samples. Table 7-1 provides the positions and lengths of the flaws as well as the position of the BET on the samples.

NDE Data Acquisition and Analysis

The samples were tested with bobbin coils and rotating probes equipped with 3 coils, a 0.115" pancake, a +Point configuration, and a 0.080" pancake. Testing was performed at 900 rpm, at an axial translation speed of 0.6" per second at a sampling rate (1000 per second) sufficient to assure that the digitization rate at the tube OD exceeded 30 per inch in both the circumferential and the axial directions; each sample was examined twice. Two analysts were employed to evaluate the data, such that two separate measurements were provided for each parameter of interest for each coil employed.

NDE Uncertainties for BET to Crack Tip Uncertainty

The distance from the bottom of the expansion transition (BET) to a crack tip requires an undegraded tube length to resist tube pullout and support leakage considerations. The NDE uncertainty on this length measurement is needed to define the total length requirement for inspection. The BET to crack tip length can be measured directly by a rotating coil probe or obtained by combining measurements for the TTS to BET and TTS to crack tip. In this study, measurements for the TTS to BET distance were made using bobbin and 115 mil coils, and TTS to crack tip measurements were made using 115 mil, 80 mil and +Point coils. For uniformity in the analysis of the eddy current data, the position of the crack tip and the location of the BET were located relative to the top of the tubesheet. To determine the uncertainty of measurement of the uppermost crack tip relative to the BET, the uncertainties of the individual measurements (TTS-BET, TTS-Crack Tip) were calculated and combined to obtain the BET to crack tip uncertainty.

The NDE uncertainties based on bobbin and 115 mil pancake coil measurements for the TTS to BET length are given under the "Direct Measurements" column in Table 7-2. Uncertainties for the TTS to an axial crack tip or a circumferential crack are dependent upon the distance from the top of the tubesheet with the uncertainties tending to increase with distance below the TTS. To reflect pullout length requirements, only indications with the crack simulations located more than 5 inches below the TTS were included in the uncertainty evaluation. The NDE uncertainties for the TTS to crack location were obtained for the 115 mil, +Point and 80 mil coils as also shown under the "Direct Measurements" column in Table 7-2. The upper 95% confidence values for the NDE uncertainties in Table 7-2 are obtained as the mean plus 1.645 times the standard deviation.

The NDE uncertainties from the direct measurements in Table 7-2 can be combined to obtain the BET to axial crack tip or circumferential crack length uncertainties. The mean error is obtained as the difference between the TTS to crack and TTS to BET mean values. The combined standard deviation is obtained as the square root of the sum of squares of the individual standard deviations. The resulting uncertainties are dependent upon whether the bobbin coil or the 115 mil coil is used to measure the TTS to BET distance due principally to differences in the mean errors for the two coils. The resulting NDE uncertainties for the distance from the BET to an axial

crack tip or to a circumferential crack at more than 5 inches below the TTS are given under the "Combined Measurements" column in Table 7-2.

The BET to crack length uncertainties at the 95% confidence level are smaller for the bobbin coil measurements than the 115 mil coil due to the difference in the mean error (positive for bobbin and negative for 115 PC). The standard deviations for the combined uncertainties are dominated by the values for the TTS to crack length measurements, which are much larger than the values for the TTS to BET length. At the upper 95% level, the BET to crack NDE uncertainties are bounded by about []^(a,c,e) for bobbin coil location of the BET and by about []^(a,c,e) for 115 mil location of the BET.

7.5 NDE CHARACTERIZATION OF TUBESHEET HOLE SURFACE ROUGHNESS

Bobbin coil testing was performed on each of the samples after all leak testing was completed. Testing was performed to emphasize tubesheet hole roughness. The bobbin coil testing provided documentation of the bobbin coil characteristics of these samples for comparison with in-generator results, if necessary.

Samples 1 and 3 were hand pulled samples, and an estimated (EST) scale was established using the tubesheet set to 8 inches (part of the tube had been pulled out of the tubesheet). Voltages were normalized to the []^(a,c) channel that was set to []^(a,c). All measurements were []^(a,c).

Table 7-3 presents a summary of the random noise measurements and Table 7-4 provides an objective ranking of the noise values as well as a subjective ranking of the noise in the graphics. It appears that all samples with noise values less than []^(a,c) are smooth bore, while those with rough bores have values greater than []^(a,c). The samples are ranked according to noise level. It is expected that a similar rank basis can be used for leakage, with leakage decreasing as bore finish roughness increases.

Table 7-4: Random Noise Sample Ranking

Sample ID	Measured Average Noise Rank From Table 7-3	Ranking Based on Noise Observed in Graphics	Tubesheet Hole Bore Type

(a,b,c)

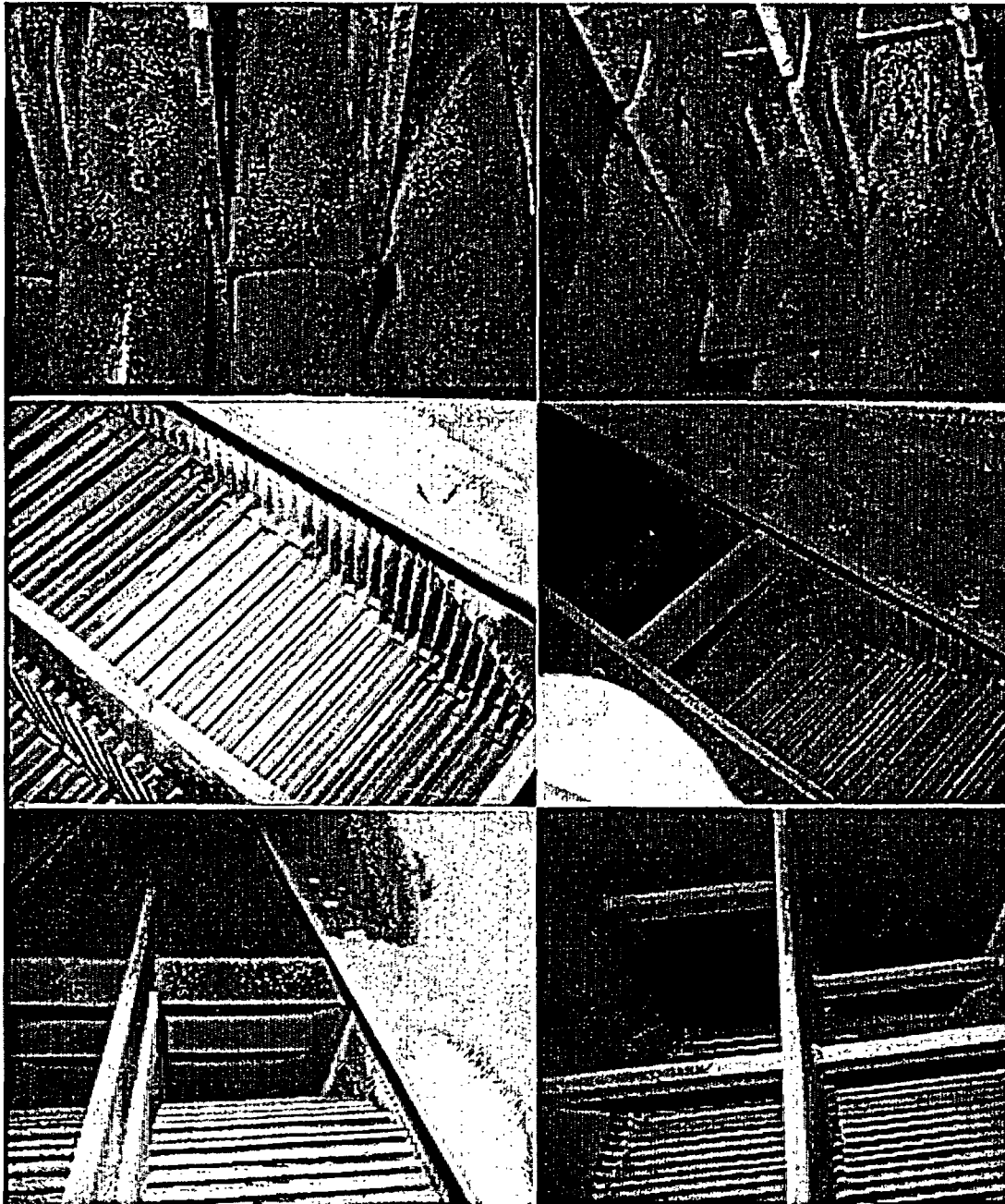


Figure 7-1: Miscellaneous Views of Upper Bundle Support Structures.

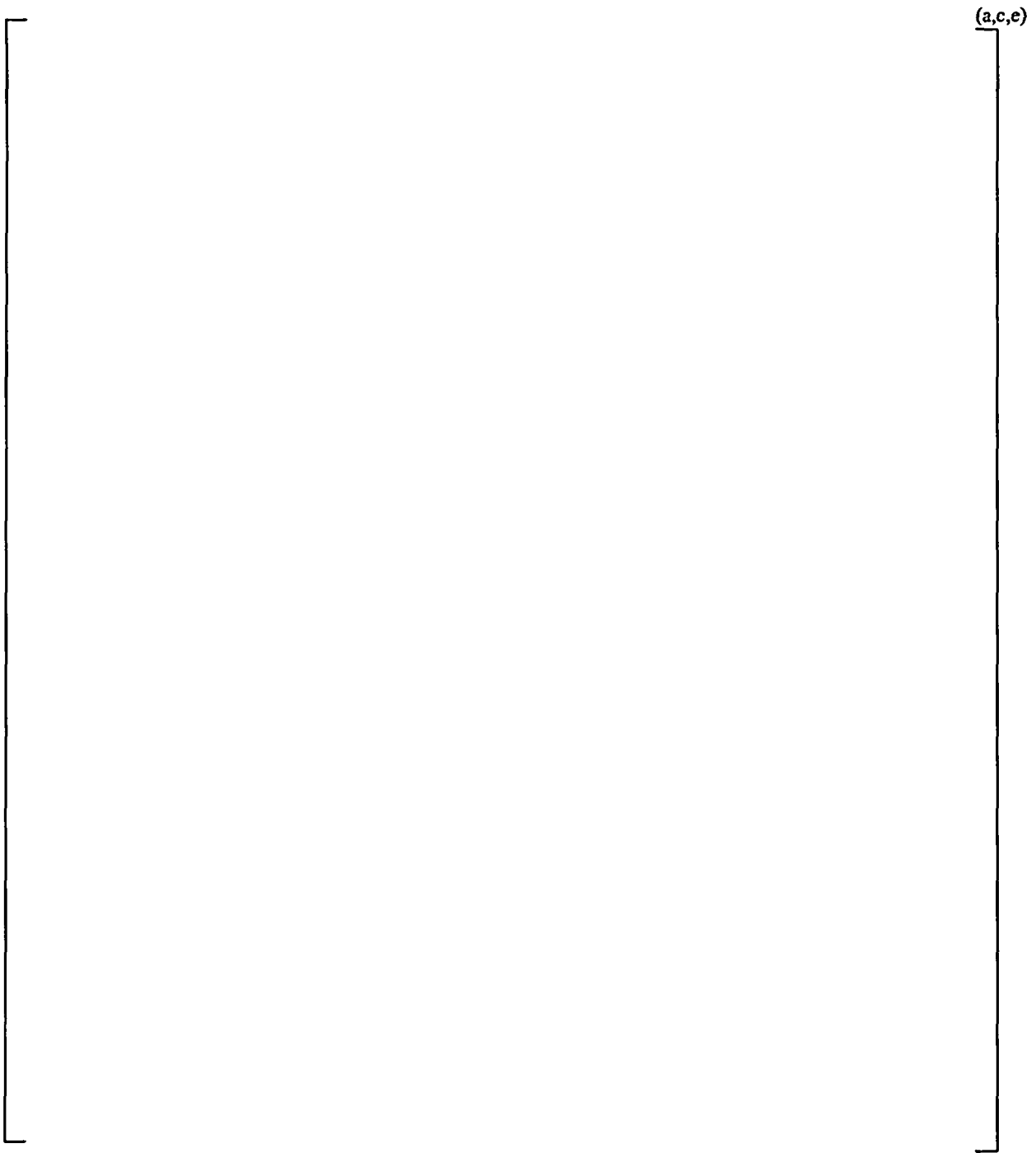


Figure 7-2: Bend Region Tube Supports.

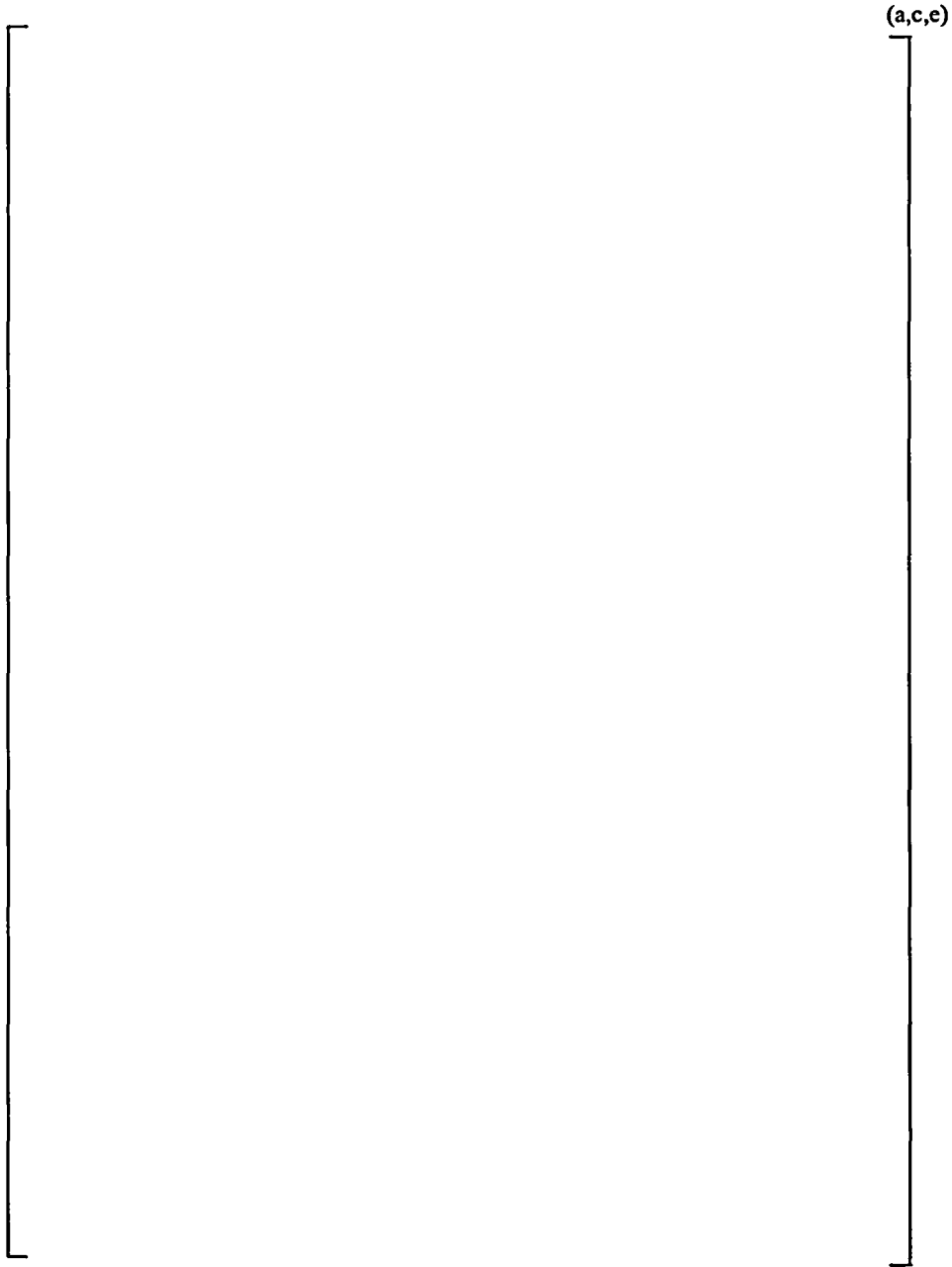


Figure 7-3: Vertical and Horizontal Strip Arrangement.

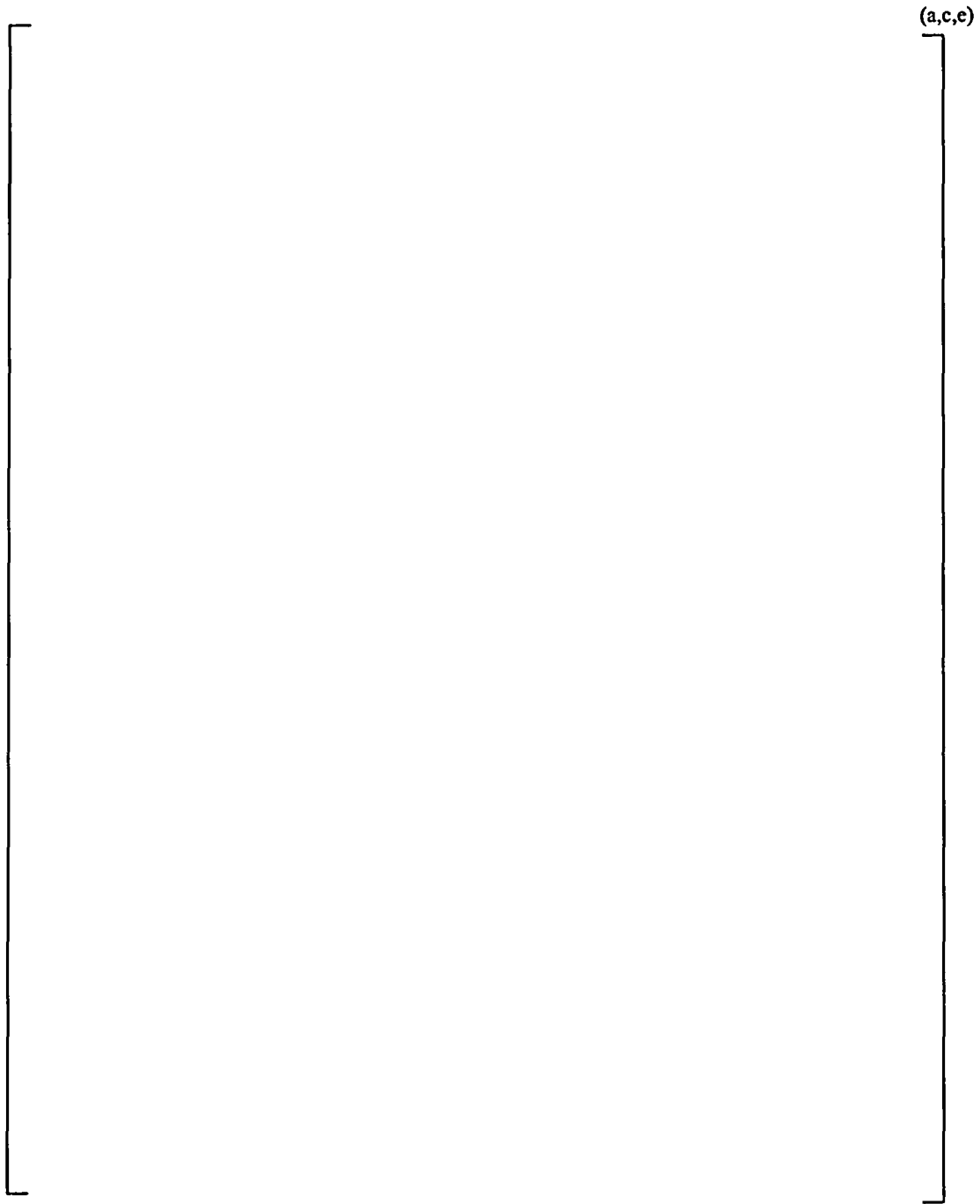


Figure 7-4: Vertical Grid Geometry.

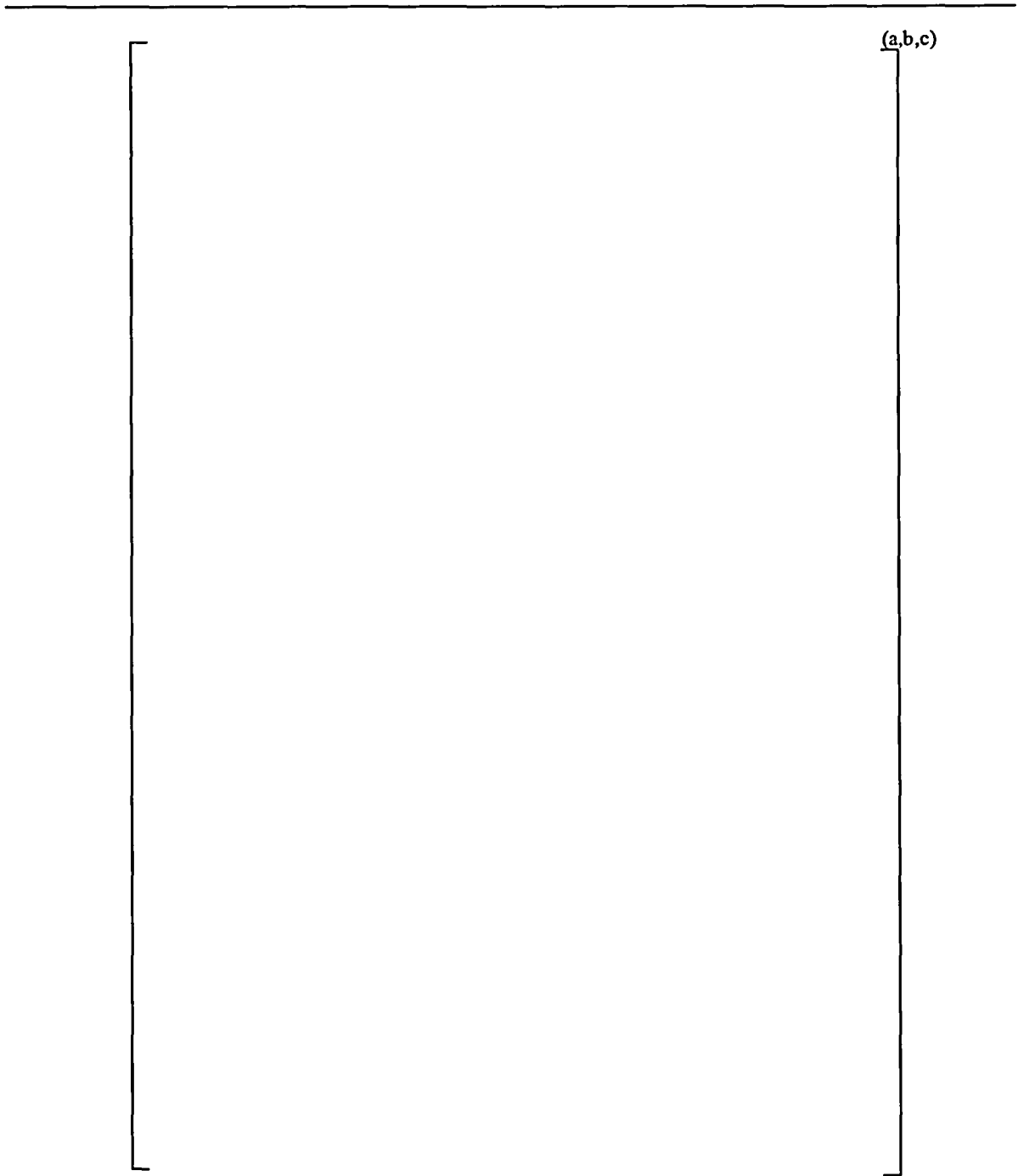


Figure 7-5: Results of EDM Cut Through the Tube Wall and Partially into the Tubesheet.

8.0 DEFINITIONS

ARC – Alternate repair criteria are approvals by NRC to utilize specific criteria for repair decisions based on detection of flaws.

BET – Bottom of the expansion transition.

BTA – Bore Trepanning Association process for machine boring. A process improvement employed for tubesheet drilling applicable to Plant CE2 (only one steam generator), Plant CE3 and the Plant CG replacement steam generators

Collar - Tubesheet mockups were fabricated from tubesheet bar stock material SA-508, Class 3. The machined bar stock in which a tube was explosively expanded was referred to in this project as a collar.

EOC – End of the operating cycle.

Expansion – Explosive expansion of tubing into a Combustion Engineering steam generator tubesheet.

Joint – The tube and tubesheet contact surface area created by the expansion process.

Leakage criteria – The criterion for tube collar testing is set at 0.1 gpm total leakage from one steam generator. The technical specifications LCO for accident induced leakage value of 0.5 gpm per steam generator is reduced by one-fifth (i.e. 0.1 gpm) to provide margin for leaks from other potential degradation types. The criterion conservatively assumes that the leakage of 0.1 gpm is from 100% of the tubes in the steam generator that have throughwall flaws present at the threshold length below the hot leg BET.

LCO – Technical specifications limiting condition for operation.

NODP – Normal operating differential pressure. RCS pressure minus SG pressure at normal full power operating conditions.

Pullout force - The force required to overcome the joint static and sliding friction such that tube movement within the tubesheet may occur.

POD – Probability of detection based on the ability of an NDE technique to indicate the presence of a flaw.

Rough Bore – The machined surface on the inside diameter of each rough bore collar was drilled on a lathe to a surface roughness not greater than 250 micro-inches (AA) to mockup the gun-drilled tubesheet hole surface.

SLB – The design basis event known as main steam line break.

Smooth Bore - The machined surface on the inside diameter of each smooth bore collar was drilled on a lathe to a surface roughness not greater than 250 micro-inches (AA) and then reamed to increase smoothness to mockup the BTA process tubesheet hole surface.

Taper – The theoretically incomplete contact near the top of the joint just below the expansion transition. The W* topical report increased the threshold length to account for an approximately 0.7” taper.

Threshold length– The tube to tubesheet joint length below the BET that provides a sufficient contact force to preclude Pullout at 3NODP and leakage at SLB pressures.

TTS – Top of the tubesheet

9.0 REFERENCES

1. "Nuclear Services Policies & Procedures," Westinghouse Quality Management System Level 2 Policies and Procedures, Westinghouse Electric Company LLC, Pittsburgh, PA, Effective 03/31/04.
2. NEI 97-06, Revision 1, "Steam Generator Program Guidelines," Nuclear Energy Institute, Washington, DC, January 2001.
3. Draft NUREG-1477, "Voltage Based Interim Plugging Criteria for Steam Generator Tubes – Task Group Report", June 2, 1993.
4. WCAP-15720 (Proprietary), Revision 0, "NDE Inspection Strategy for Tubesheet Regions in CE Designed Units," CEOG Task 1154, Westinghouse Electric Company LLC, Windsor, CT, July 2001.
5. Generic Letter 2004-01, "Requirements for Steam Generator Tube Inspections," United States Nuclear Regulatory Commission, Washington, DC, August 30, 2004.
6. Valinox Nucleaire, Certified Material Test Report, Heats NX8520, NX9915, Certificate 9713971, July 28, 1997.
7. Test Procedure, 00-TP-FSW-001, Revision 01 (Proprietary), "Procedure for Testing Steam Generator Tubes for Leakage Within the Tubesheet," Westinghouse Electric Company, Windsor, CT, February 15, 2000.
8. TP-SGDA-03-3 (Proprietary), "Procedure for Leak and Pullout Testing of C* Samples," Westinghouse Electric Company LLC, Windsor, CT, 2003.
9. TR-1007904-R2, "Steam Generator in Situ Pressure Test Guidelines," Revision 2, EPRI, Palo Alto, CA, August 2003.
10. TP-SGDA-04-1 (Proprietary), Revision 1, "Testing to Compare Leak Test Water Chemistry," Westinghouse Electric Company LLC, Pittsburgh, PA, April 15, 2004.
11. ASME Steam Tables, Revision 6, American Society of Mechanical Engineers, New York, New York, 1967.
12. CENC-1272 (Proprietary), Analytical Report for SCE San Onofre Unit No. 2 Steam Generators, Westinghouse Electric Company LLC, Windsor, CT, September 1976.
13. WCAP-13532 (Proprietary), Revision 1, "Sequoyah Units 1 and 2 W* Tube Plugging Criteria fro SG Tubesheet Region of WEXTEx Expansions," Westinghouse Electric Company LLC, Pittsburgh, PA, November 1992.
14. NRC GL 95-05, "Voltage-Based Repair Criteria for Westinghouse Steam Generator Tubes Affected by Outside Diameter Stress Corrosion Cracking", August 3, 1995.
15. WCAP-14046, "Braidwood Unit 1 Technical Support for Cycle 5 Steam Generator Interim Plugging Criteria", May 1994.

16. NRC Safety Evaluation Report, "Issuance of Amendment No. 50 to Facility Operating License NPF-72, Braidwood Station, Unit 1 (TAC No. M89166), May 7, 1994.
17. STD-DA-04-16, "Statistical Analysis of C*, Task 1154, W* and H* Data (revised)," Westinghouse Electric Company LLC, Churchill, PA, September 14, 2004.
18. "Perry's Chemical Engineers' Handbook," Sixth Edition, McGraw-Hill, New York, New York, USA, 1984.
19. B. Efron, and R.J. Tibshirani, "An Introduction to the Bootstrap," Chapman and Hall, 115 Fifth Avenue, New York, New York, USA, 1993.
20. WCAP-14277, "SLB Leak Rate and Tube Burst Probability Analysis Methods for ODSCC at TSP Intersections," Westinghouse Electric Company LLC, Madison, PA, December 1996.
21. Regulatory Guide 1.121 (Draft), Bases for Plugging Degraded PWR Steam Generator Tubes," United States Nuclear Regulatory Commission, Washington, DC, August 1976 (issued for comment).
22. WCAP-15894-P (Proprietary), Supplement 1, "Supplement to NDE Inspection Strategy for the Tubesheet Region in SONGS Units 2 and 3," Westinghouse Electric Company LLC, Windsor, CT, November 2002.
23. CN-SGDA-03-73 (Proprietary), Revision 1, "Effects of Tubesheet Flexure on Tube Pullout Loads in CE-Designed Steam Generators for SONGS 2 & 3, St. Lucie 2, Ft. Calhoun, Waterford 3, Palisades and Palo Verde 1, 2, & 3 Plants" Westinghouse Electric Company LLC, Windsor, CT, 2003.
24. WCAP-14797-P (Proprietary), Revision 2, "Generic W* Plugging Criteria for 51 Series Steam Generator Tubesheet Region WEXTEx Expansions," Westinghouse Electric Company LLC, Madison, PA, March 2003.
25. WCAP-16159-P (Proprietary), "Justification for the Partial-Length Rotating Pancake Coil (RPC) Inspection of the Tube Joints of the Seabrook Unit 1 Model F Steam Generators," Westinghouse Electric Company LLC, Madison, PA, September 2003.
26. W. C. Young and R. G. Budynas, "Roark's Formulas for Stress and Strain," Seventh Edition, Mc-Graw-Hill, New York, New York, 2002.
27. J. N. Goodier and G. J. Schoessow, "The Holding Power and Hydraulic Tightness of Expanded Tube Joints: Analysis of the Stress and Deformation," Transactions of the ASME, Volume 65, pp. 489-496, American Society of Mechanical Engineers, New York, New York, July 1943.

APPENDIX A

Summary of Room Temperature Leak Test Results

APPENDIX B

Summary of Elevated Temperature Leak Test Results

APPENDIX C
LEAK RATE VS TIME PLOTS AT SLB

Leak Rate vs. Time (Sample 1, $x=3''$, $P=SLB$)



Leak Rate vs. Time (Sample 2, x=3", P=SLB)

(a,b,c)



Leak Rate vs. Time (Sample 2, x=2", P=SLB)



Leak Rate vs. Time (Sample 2, x=1.5", P=SLB)



Leak Rate vs. Time (Sample 3, x=4", P=SLB)

(a,b,c)



Leak Rate vs. Time (Sample 3, x=3", P=SLB)



Leak Rate vs. Time (Sample 3, x=2", P=SLB)



Leak Rate vs. Time (Sample 4, x=4", P=SLB)



Leak Rate vs. Time (Sample 4, x=3", P=SLB)

(a,b,c)



Leak Rate vs. Time (Sample 5, x=3", P=SLB)

(a,b,c)



Leak Rate vs. Time (Sample 5, $x=2.5''$, $P=SLB$)



Leak Rate vs. Time (Sample 6, x=2.25", P=SLB)

(a,b,c)



Leak Rate vs. Time (Sample 7, x=3", P=SLB)



Leak Rate vs. Time (Sample 7, x=2", P=SLB)



Leak Rate vs. Time (Sample 36, x=5.5", P=SLB)



Leak Rate vs. Time (Sample 36, x=3.5", P=SLB)



Leak Rate vs. Time (Sample 37, $x=5.5"$, P=SLB)

